

# Polyakov Loop Dynamics in the Center Symmetric Phase

F. Lenz and M. Thies

*Institute for Theoretical Physics III, University of Erlangen-Nürnberg,  
Staudtstr. 7, 91058 Erlangen, Germany*

## Abstract

A study of the center symmetric phase of  $SU(2)$  Yang Mills theory is presented. Realization of the center symmetry is shown to result from non-perturbative gauge fixing. Dictated by the center symmetry, this phase exhibits already at the perturbative level confinement like properties. The analysis is performed by investigating the dynamics of the Polyakov loops. The ultralocality of these degrees of freedom implies significant changes in the vacuum structure of the theory. General properties of the confined phase and of the transition to the deconfined phase are discussed. Perturbation theory built upon the vacuum of ultralocal Polyakov loops is presented and used to calculate, via the Polyakov loop correlator, the static quark-antiquark potential.

# 1 Introduction

Confinement of the elementary degrees of freedom is a fundamental property of Quantum Chromodynamics (QCD). It has been subject of many investigations, and a variety of mechanisms have been proposed for its explanation. Here we mention as particularly relevant for our present work the restriction in the range of the functional integration due to the presence of Gribov horizons in gauge fixed formulations [1], or the appearance and possible condensation of magnetic monopoles in Abelian projected descriptions [2]. Despite considerable analytical and numerical efforts and largely due to the gauge dependence of most of the discussed mechanisms, no definite picture has yet emerged nor have interrelations between these mechanisms been established.

The focus of our study of the confining phase of QCD will be on the center symmetry [3, 4, 5] and the associated order-fields, the Polyakov loop variables [6, 7, 8]. Irrespective of the details of the dynamics which give rise to confinement, this symmetry must be realized in the confining and spontaneously broken in the “quark-gluon plasma” phase. Unlike in lattice gauge calculations, the issue of the center symmetry has essentially played no role in analytical investigations so far. In general, perturbative calculations break this symmetry and thus inevitably are guided towards the deconfined phase. This is due to the change of the underlying gauge symmetry from  $SU(N)$  to  $U(1)^{N^2-1}$  when the coupling vanishes. In this limit, the original  $Z_N$  symmetry gets effectively broken. For the center symmetry to be preserved in the path integral formulation, the Faddeev–Popov determinant [9] arising in the process of gauge fixing cannot be treated perturbatively. In particular the associated restrictions in the range of integrations which prevent summation over Gribov copies cannot be neglected. Likewise, for the center symmetry to be preserved in the canonical formalism, the Gauss law has to be resolved non-perturbatively. Only then the center symmetry is guaranteed to appear as the correct residual gauge symmetry.

For the formulation of the center symmetry and definition of the Polyakov loops we consider QCD at finite extension, i.e., in a geometry where the system is of finite extent ( $L$ ) in one direction ( $x_3$ ), but of infinite extent in the other directions (coordinates denoted by  $x_\perp = (x_0, x_1, x_2)$ ). Choosing one compact coordinate is of interest for additional reasons. First, the parameter  $L$  helps to control infrared ambiguities. This is of particular importance when using axial like gauges (for an early discussion of ambiguities in the axial gauge, see Ref. [10]). Second, by covariance, QCD at finite extension is equivalent to finite temperature QCD and, therefore, the essential properties of finite extension QCD are known from finite temperature lattice gauge calculations (for a recent review, cf. [11]). In particular the presence of a phase transition at finite temperature implies, via covariance, occurrence of a phase transition when compressing the system, i.e., decreasing  $L$ . It also implies dimensional reduction to 2 + 1 dimensional QCD to occur [12, 13] if the system is compressed far beyond the typical length scale of strong interaction physics. Although identification of the compact direction with imaginary time is more familiar, we will use the finite extension interpretation by making a spatial direction compact. In this case, the canonical formulation is straightforward, and the center symmetry plays the role of an ordinary symmetry.

The variables of central importance in our investigation of the center symmetry are the Polyakov loops winding around the compact 3-direction. These variables characterize the phases of QCD (cf. [8] for finite temperature QCD), in particular the realization of the center symmetry in the absence of quarks. Thereby they serve as order parameters of the confinement-deconfinement transition occurring at a certain critical extension.

Besides the choice of the geometry, the choice of gauge is the second important technical ingredient on which our investigations are based. With one of the space-time directions made compact, the use of an axial type gauge seems natural. Moreover in such a gauge the Polyakov loop variables appear as elementary rather than composite degrees of freedom. This makes the whole setting particularly appropriate for a study of the center symmetry and of the dynamics of the Polyakov loops. Indeed the center symmetry will remain present at each level of the theoretical development. This is possible only because the elimination of redundant variables can be performed in closed form without invoking at any step perturbation theory.

Realization of the center symmetry implies the presence of novel structural elements as compared to standard perturbative QCD. In particular, the center symmetric phase with its infinite energies associated with single static color charges does not exhibit, as might be expected, the phenomenon of (chromo-electric) Debye screening [14]. Rather, naive application of perturbation theory will be seen to lead to tachyonic behaviour of the Polyakov loop variables. This perturbative instability indicates qualitative changes in the structure of the vacuum which will be shown to arise from the ultralocality of the Polyakov loops. Ultralocality, i.e., the missing strength to generate wave phenomena, represents an extreme form of confinement of these degrees of freedom. This property will provide an appropriate framework for the discussion of a variety of non-perturbative, confinement related phenomena. On the other hand, these drastic deviations in the Polyakov loop vacuum from the perturbative one necessarily obscure the standard short distance perturbative properties of QCD. This dichotomy between perturbative and non-perturbative physics will be illustrated by a detailed discussion of the interaction energy of static quarks. In this approach to the Polyakov loop dynamics, certain non-perturbative infrared properties are almost trivial consequences of the vacuum structure, while description of the short distance, Coulomb-like behaviour will be seen to require coupling of Polyakov loops to other gluonic variables to infinite order.

Aside from the Introduction and Conclusions, this paper is organized into three main sections. In Sect. 2, the QCD generating functional is derived in a modified axial gauge, using a space with finite extension in the 3-direction. Path integral quantization is used to rederive in a self-contained and streamlined fashion results of our earlier canonical studies (Sect. 2.2), the main emphasis being on the SU(2) case (Sect. 2.3). We have also included a brief reminder on the equivalence of finite temperature and finite extension field theory (Sect. 2.1) and illustrated the difficulties encountered in the evaluation of screening effects, if one tries to treat the Faddeev–Popov determinant perturbatively (Sect. 2.4). Section 3 addresses the issue of Polyakov loops and exhibits ultralocality as their main characteristics. In Sect. 3.2, we show how one can make use of this property of the Polyakov loops to integrate them out, thereby deriving an effective theory for the other degrees of freedom which admits a continuum limit. A qualitative discussion of the

phases of QCD (Sect. 3.3) and the confinement-deconfinement transition (Sect. 3.4), as they appear in this novel description, follow. Sect. 4 summarizes our efforts to use the effective theory for investigating properties of the center symmetric phase with the help of perturbation theory, which now is markedly different from standard perturbation theory. Feynman rules are given (Sect. 4.1) and the gluon two-point function (Sect. 4.3) and Polyakov loop correlator at one (Sect. 4.2) and two loop level (Sect. 4.4) are discussed in detail, emphasizing the short distance aspects. These investigations are then used to gain insight into the interaction between static quarks (Sect. 4.5) as well as shielding effects in the presence of dynamical quarks (Sect. 4.6). The two appendices contain material of technical nature referred to in the main text, namely the calculation of the electron self energy in axial gauge QED (Appendix A) and the full expressions for the one loop gluon self energy in modified axial gauge QCD (Appendix B).

## 2 QCD in the Axial Gauge

### 2.1 Finite Extension versus Finite Temperature

Before developing the formalism for axial gauge QCD we briefly discuss the relation between QCD at finite extension and finite temperature. The equivalence of relativistic field theories at finite extension and finite temperature has been noted in Ref. [15] and used e.g. in a discussion of the finite temperature quark propagators [16]. By rotational invariance in the Euclidean, the value of the partition function of a system with finite extension  $L$  in 3 direction and  $\beta$  in 0 direction is invariant under the exchange of these two extensions,

$$Z(\beta, L) = Z(L, \beta) , \quad (1)$$

provided bosonic (fermionic) fields satisfy periodic (antiperiodic) boundary conditions in both time and 3 coordinate. Thus relativistic covariance connects the thermodynamic properties of a canonical ensemble with the properties of the pure state of the vacuum corresponding to the same physical system but at finite extension. In particular, as a consequence of (1), energy density and pressure are related by

$$\epsilon(\beta, L) = -p(L, \beta) . \quad (2)$$

For a system of non-interacting particles this relation connects energy density or pressure of the Stefan Boltzmann law with the corresponding quantities measured in the Casimir effect.

In QCD, by covariance, the existence of a phase transition at finite temperature implies the occurrence of a phase transition when compressing the QCD vacuum (i.e., decreasing  $L$ ). From this point of view, the confinement-deconfinement phase transition or the chiral phase transition, when quarks are present, appear as “quantum phase transitions” (cf. [17], [18]). They are driven by changes in quantum rather than thermal fluctuations which in turn are induced by changes of a parameter of the system ( $L$ ). Covariance connects quantitatively compressed and heated systems with each other. In particular, we conclude

from Eq. (2) that in the phase transition induced by compressing the system the Casimir pressure changes discontinuously, while the change in the energy density is continuous. Furthermore, from results of lattice gauge calculations [11], we infer that this transition occurs at a critical extension  $L_c \approx 0.8$  fm in the absence of quarks and at  $L_c \approx 1.3$  fm when quarks are included. These typical length scales indicate that we do not have to treat the extension strictly as an infrared parameter which tends to infinity. Rather we expect no essential property of the QCD vacuum to be changed significantly if  $L$  is of the order of 2–3 fm. For extensions smaller than  $L_c$ , the energy density and pressure reach values which are typically 80 % of the corresponding “Casimir” energy and pressure. If the system is compressed further and the extension becomes much smaller than typical length scales of strong interaction physics (e.g. a typical hadron radius  $R$ ), we expect correlation functions at transverse momenta or energies  $|p| \ll 1/L$  to be dominated by the zero “Matsubara wave numbers” in 3-direction and thus to be given by the dimensionally reduced QCD<sub>2+1</sub>. Lattice calculations [19] provide evidence for this dimensional reduction to occur if one of the Euclidean extensions becomes small.

The variables of central importance in our investigation of the role of the center symmetry are the Polyakov loops winding around the compact 3-direction

$$\mathcal{P}(x_\perp) = N_c^{-1} \text{tr} \text{P exp} \left\{ ig \int_0^L dx_3 A_3(x) \right\}. \quad (3)$$

The vacuum expectation values of  $\mathcal{P}$  characterizes the phases of QCD (cf. [8] for finite temperature QCD), in particular their realization of the center symmetry in the absence of quarks. Thereby they serve as order parameters of the confinement-deconfinement transition occurring when varying the extension.

## 2.2 The Generating Functional

For the theoretical treatment of QCD at finite extension or finite temperature an axial type gauge is particularly appropriate. In such gauges, the associated Polyakov loops appear as fundamental rather than composite degrees of freedom; this in turn permits a direct study of the dynamics of the order parameter for the confinement-deconfinement transition. The derivation of the axial gauge representation and a discussion of the subtleties associated with this gauge choice has been carried out already within the canonical formalism [20, 21]. Here we rewrite these results into the path-integral formulation which serves as the basis for the following developments (a related discussion is given in Ref. [22]). The formal expression for the QCD generating functional after gauge fixing is

$$Z = \int d[A, \psi, \bar{\psi}] e^{iS_{\text{QCD}}[A, \psi, \bar{\psi}]} \Delta_{\text{FP}}[A] \delta[f[A]] \quad (4)$$

with the standard QCD action

$$S_{\text{QCD}}[A, \psi, \bar{\psi}] = \int d^4x \left\{ -\frac{1}{4} F^{a\mu\nu} F_{\mu\nu}^a + \bar{\psi} (i\not{D} - m) \psi \right\}. \quad (5)$$

We require gluon and quark fields to satisfy periodic and antiperiodic boundary conditions respectively,

$$\begin{aligned} A_\mu^a(x_\perp, x_3 = L) &= A_\mu^a(x_\perp, x_3 = 0) , \\ \psi(x_\perp, x_3 = L) &= \psi(x_\perp, x_3 = 0) , \end{aligned} \quad (6)$$

with the notation

$$x = (x_\perp, x_3) .$$

This choice of boundary conditions is necessary for the equivalence of finite extension and finite temperature formulations. Covariant derivative  $D$  and field strength tensor  $F$  are defined as usual,

$$\begin{aligned} D_\mu &= \partial_\mu + igA_\mu , \\ F_{\mu\nu} &= \partial_\mu A_\nu - \partial_\nu A_\mu + ig[A_\mu, A_\nu] . \end{aligned} \quad (7)$$

Gauge fixing is implicitly described by the  $\delta$ -functional and the corresponding Faddeev–Popov determinant in Eq. (4) and is carried out explicitly in two steps. First, the functional integral is constrained by the following choice of  $f$ ,

$$f_x^a[A] = A_3^a(x) (1 - \epsilon^a) + \eta \partial_3 A_3^a \epsilon^a , \quad (8)$$

where  $\epsilon^a=1$  (0) if  $a$  refers to a diagonal (non-diagonal)  $\lambda$  matrix. The Faddeev–Popov determinant associated with this gauge choice is determined by

$$\delta[f[A]] \mathcal{M}(x, y; a, b) = -\delta[f[A]] \left( \partial_3^y \delta^{ab} (1 - \epsilon^a + \eta \epsilon^a \partial_3^x) - g f^{abc} \epsilon^c A_3^c(y_\perp) \right) \delta^4(x - y) . \quad (9)$$

The matrix  $\mathcal{M}$  factorizes into contributions from “neutral” gluons ( $\epsilon^a = \epsilon^b = 1$ ) which are independent of the gauge fields and from “charged” gluons ( $\epsilon^a = \epsilon^b = 0$ ) which give rise to a non-trivial Faddeev–Popov determinant  $\det(\mathcal{M})$ ,

$$\delta[f[A]] \mathcal{M}(x, y; a, b) = -\delta[f[A]] \left( \partial_3^y \delta^{ab} - g \epsilon^c f^{abc} A_3^c(y_\perp) \right) \delta^4(x - y) . \quad (10)$$

The Faddeev–Popov determinant is given by the product of eigenvalues of the covariant derivative  $D_3$

$$\left( \partial_3 \delta^{ab} - g \epsilon^c f^{abc} A_3^c(x_\perp) \right) \Psi^b(x) = i\mu \Psi^a(x) \quad (11)$$

which can be calculated explicitly,

$$\mu_{p,q,n}(x_\perp) = \frac{2\pi n}{L} + g(A_3^{qq}(x_\perp) - A_3^{pp}(x_\perp)) , \quad (12)$$

yielding

$$\Delta_{\text{FP}} = \prod_{p,q,n,x_\perp} \mu_{p,q,n}(x_\perp) \sim \prod_{p>q,x_\perp} \sin^2 \left[ \frac{gL}{2} (A_3^{qq}(x_\perp) - A_3^{pp}(x_\perp)) \right] . \quad (13)$$

The gauge fixing by Eq. (8) is not complete; Abelian,  $x_3$  independent gauge transformations leave the integrand in Eq. (4) invariant. In a second step a residual gauge condition

can be imposed. For perturbative applications a 2+1 dimensional Lorentz gauge condition is implemented via a gauge fixing term in the action,

$$S_{\text{gf}}[A] = - \sum_{c_0=1}^{N-1} \int d^4x \frac{1}{2\xi} \left( \frac{1}{L} \int_0^L dx_3 \partial^\mu A_\mu^{c_0} \right)^2. \quad (14)$$

The sum extends over the neutral gluons only. As in electrodynamics, no field dependent Faddeev–Popov determinant arises from this residual gauge fixing (within the canonical formalism implementation of a residual Coulomb gauge constraint is more natural, cf. [20]).

Thus the generating functional of QCD in the axial gauge can be written in the following form,

$$Z = \int d[\psi, \bar{\psi}] \prod_{\mu=0}^2 d[A_\mu] \prod_{c_0=1}^{N-1} d[A_3^{c_0}] \Delta_{\text{FP}}[A] e^{i(S[A, \psi, \bar{\psi}] + S_{\text{gf}}[A])}. \quad (15)$$

The 3-components of the gauge fields have been eliminated up to 2+1 dimensional, neutral fields. Apart from the longitudinal, 2+1 dimensional, neutral gluon fields which appear in the gauge fixing term, no redundant degrees of freedom are present anymore.

## 2.3 QCD with SU(2) Color

We analyse the formal structure of the generating functional in the context of SU(2)-QCD. This discussion will provide the basis for our dynamical studies. In comparison to a naive axial gauge formulation, the distinctive element in the generating functional (15) is the presence of the Faddeev–Popov determinant (Eq. (13)) which for SU(2) is given by

$$\Delta_{\text{FP}} = \prod_{x_\perp} \sin^2 \left( gLA_3^{11}(x_\perp) \right). \quad (16)$$

Gauge fields with polarization in the 3-direction cannot be eliminated completely; the eigenvalues of the Polyakov loops winding, for fixed  $x_\perp$ , around the compact 3 direction are gauge invariant objects and therefore have to be kept. The Faddeev–Popov determinant (Eqs. (13), (16)) is given by the Haar measure associated with these particular group elements which, in SU(2), is the volume element of the first polar angle in the parametrization of the group manifold by polar coordinates. It is thus clear that the Faddeev–Popov determinant implicitly contains a restriction to a finite range of integration — the fundamental domain determined by the zeroes of  $\Delta_{\text{FP}}$ . For SU(2), this is the finite interval  $[0, \pi]$  of definition of the polar angle  $gLA_3^{11}$ .

The presence of the Faddeev–Popov determinant with its restriction in the range of integration poses serious problems in defining the weak coupling limit as the basis for perturbation theory. In the standard treatment, the variables  $a_3$  are taken as Gaussian variables with the real axis as range of definition, and the Faddeev–Popov determinant is effectively neglected. Expansion of action and Faddeev–Popov determinant around  $a_3 = 0$  is however problematic; at this point  $\Delta_{\text{FP}}$  vanishes and therefore yields a singular contribution to the (effective) action. The meaning of results obtained within such

a framework such as the electric screening mass is not quite obvious. The subtleties of the weak coupling limit in this gauge are related to the change in symmetry from  $SU(N)$  to  $U(1)^{N^2-1}$  occurring at  $g = 0$ . Concomitant with this change in symmetry is a change from the  $N - 1$  gauge invariant eigenvalues of the Polyakov loops at finite  $g$  to the  $N^2 - 1$  ( $U(1)$  gauge invariant) “zero-mode” photons at  $g = 0$ . For the following it is convenient to introduce the “Polyakov loop variables”

$$a_3(x_\perp) = 2A_3^{11}(x_\perp) - \frac{\pi}{gL} \quad (17)$$

and to redefine accordingly charged gluon and quark fields,

$$\begin{aligned} A_\mu^{pq}(x) &\rightarrow \exp\left[-ix_3 \frac{\pi}{2L} ((\tau_3)_{qq} - (\tau_3)_{pp})\right] A_\mu^{pq}(x) , \\ \psi(x) &\rightarrow \exp\left[-ix_3 \frac{\pi}{2L} \tau_3\right] \psi(x) . \end{aligned} \quad (18)$$

In this way, the standard form of the action is preserved and the  $SU(2)$ -QCD generating functional given by

$$Z = \int d[\psi, \bar{\psi}] \prod_{\mu=0}^2 d[A_\mu] d[a_3] \Delta_{\text{FP}}[a_3] e^{i(S[A_\perp, a_3, \psi, \bar{\psi}] + S_{\text{gf}}[A_\perp^3])} , \quad (19)$$

with the Faddeev–Popov determinant

$$\Delta_{\text{FP}}[a_3] = \prod_{x_\perp} \cos^2(gLa_3(x_\perp)/2) . \quad (20)$$

For perturbative calculations it might be advantageous to represent this determinant as a functional integral over (anticommuting) ghost fields

$$e^{iS_{\text{FP}}} = \int d[c, c^\dagger] e^{iS_{\text{gh}}[c, c^\dagger]} \quad (21)$$

with

$$S_{\text{gh}} = \int d^4x c_a^\dagger(x) \left( \frac{1}{i} \partial_3 \delta^{ab} + ig\epsilon^{3ab} a_3(x_\perp) \right) c_b(x) . \quad (22)$$

Finally we observe that due to the explicit  $x_3$ -dependence of the above field redefinitions and a similar treatment of the ghost fields, changes in the boundary conditions occur,

$$\begin{aligned} A_\mu^a(x_\perp, x_3 = L) &= (-1)^{1+\epsilon_a} A_\mu^a(x_\perp, x_3 = 0) \\ c_a(x_\perp, x_3 = L) &= -c_a(x_\perp, x_3 = 0) \\ \psi(x_\perp, x_3 = L) &= e^{-i\pi\tau_3/2} \psi(x_\perp, x_3 = 0) , \end{aligned} \quad (23)$$

i.e., neutral gluons remain periodic while charged gluons and ghosts satisfy antiperiodic boundary conditions. Quark fields acquire a phase  $\pi/2$  in going around the compact 3-direction. These changes in the boundary condition will have important consequences. We emphasize at this point that we have not modified the basic requirements of periodicity or antiperiodicity (Eq. (6)) for boson and fermion fields, respectively.

In the axial gauge, with the Polyakov loops chosen to point in color 3 direction, charged and neutral gluons are dynamically distinguished as in any form of ‘‘Abelian projection’’. In such a formulation of QCD it often is convenient to use charged instead of cartesian color components,

$$\Phi_\mu(x) = \frac{1}{\sqrt{2}} \left( A_\mu^1(x) - iA_\mu^2(x) \right) \quad \mu = 0, 1, 2 . \quad (24)$$

In terms of these charged gluon fields the center ( $Z_2$ ) symmetry transformation which, in the absence of dynamical quarks, leaves the generating functional invariant

$$C : \begin{aligned} a_3(x_\perp) &\rightarrow -a_3(x_\perp) \\ A_\mu^3(x) &\rightarrow -A_\mu^3(x) \\ \Phi_\mu(x) &\rightarrow \Phi_\mu^\dagger(x) , \end{aligned} \quad (25)$$

is the charge conjugation. We furthermore note that the Polyakov loop is given by

$$\mathcal{P}(x_\perp) = \text{tr} \text{P} e^{ig \int_0^L dz A^3(x_\perp, z)} = \sin(gLa_3(x_\perp)/2) \quad (26)$$

(in  $SU(2)$ ,  $\mathcal{P}(x_\perp)$  is hermitean so that there is no distinction between static quarks and antiquarks). In the confined phase, at extensions  $L > L_c$ , charge conjugation symmetry is realized

$$C|0\rangle = \pm|0\rangle , \quad (27)$$

with vanishing Polyakov loop expectation value. The ground state of the deconfined phase at  $L < L_c$  with its non-vanishing Polyakov loop expectation value breaks spontaneously charge conjugation symmetry.

## 2.4 Anti-Screening

Before continuing with the development of the formalism we present a preliminary perturbative analysis of screening properties associated with Polyakov loops. The relevant quantity to be calculated is the 33-component of the polarization tensor  $\Pi_{33}$  which, to lowest order and in the absence of dynamical quarks, is given by the sum of tadpole, ghost and two gluon diagrams of Fig. 1. The intermediate charged gluon propagators of the tadpole (1a) and gluon loop (1c) diagrams and the ghost propagator of diagram (1b) are given by

$$\begin{aligned} D_{\mu\nu}^{ab}(p) &= \delta^{ab} \frac{1}{p^2 - p_3^2 + i\epsilon} \left[ -g_{\mu\nu} + \frac{p_\mu p_\nu}{p_3^2} \right] \\ \Delta^{ab}(p) &= \delta^{ab} \frac{1}{p_3} . \end{aligned} \quad (28)$$

The discrete values of the 3-component of the momenta are

$$p_{3,n} = (2n + 1) \frac{\pi}{L} . \quad (29)$$

According to the ghost contribution to the action (Eq. (22)), the ghost-Polyakov loop vertex is given by

$$V_{\text{ghP}} = -g\epsilon^{3ab} \quad (30)$$

with the color labels  $a, b$  of the ghost fields. Here and in the following, Greek indices denote the components 0,1,2, and correspondingly we use the notation

$$p^2 = p^\mu p_\mu = p_0^2 - p_1^2 - p_2^2 .$$

For our qualitative discussion of screening, we consider the simple case of vanishing Polyakov loop momentum and obtain

$$\Pi_{33}(0) = 2g^2 \frac{1}{L} \sum_{n=-\infty}^{\infty} \int \frac{d^3 p}{(2\pi)^3} [m_{\text{tp}}(p) + m_{\text{gh}}(p) + m_{\text{gg}}(p)] , \quad (31)$$

with the following contributions from the 3 diagrams,

$$\begin{aligned} m_{\text{tp}}(p) &= -\frac{1}{p_{3,n}^2} + \frac{2}{p^2 - p_{3,n}^2 + i\epsilon} \\ m_{\text{gh}}(p) &= \frac{1}{p_{3,n}^2} \\ m_{\text{gg}}(p) &= \frac{2}{p_{3,n}^2} + \frac{4p_{3,n}^2}{(p^2 - p_{3,n}^2 + i\epsilon)^2} \end{aligned} \quad (32)$$

The integral in Eq. (32) is performed with the help of dimensional regularization,

$$\Pi_{33}(0) = \frac{i2g^2}{\pi L} \sum_{n=-\infty}^{\infty} \sqrt{p_{3,n}^2} , \quad (33)$$

and the divergent sum is computed in  $\zeta$ -function regularization with the final result

$$\Pi_{33}(0) = \frac{1}{3} \frac{ig^2}{L^2} . \quad (34)$$

To appreciate the relevance of this result, we remark that in our regularization procedure the ghost loop does not contribute at all; the ghost propagator depends on the 3-component of the momentum only and, in 3 dimensions, the rules of dimensional regularization imply

$$\int \frac{d^3 p}{(2\pi)^3} = 0 . \quad (35)$$

This result can be generalized to show that the ghost-gluon coupling has no effect whatsoever to any order. We consider as an example the diagram of Fig. 2. Neither the ghost-Polyakov loop vertices nor the propagators depend on the (0,1,2)-components of the loop momentum  $p$ , and therefore such diagrams involving ghost loops vanish. This suggests that no effects of the Faddeev–Popov determinant are seen in perturbation theory, and one might be tempted to drop the corresponding contribution to the action in Eq. (19). In this case, one could equally well try to define perturbation theory using

the original variable  $A_3^{11}(x_\perp)$ . In our screening calculation the only change concerns the values of the 3-components of the charged gluon momenta which are now determined by periodic boundary conditions. Unfortunately a proper definition of the charged gluon propagator is not possible due to the presence of a zero mode in the quadratic part of the charged gluon contribution to the action (the gauge term in the first line of Eq. (28) is not defined for  $p_3 = 0$ ). Disregarding for the moment this difficulty and excluding 0 from the momentum sum, we obtain the same formal expression for the polarization tensor as above with the momenta  $p_{3,n}$  summed over the values  $2n\pi/L$ . The final result is

$$\tilde{\Pi}_{33}(0) = -\frac{2ig^2}{3L^2} . \quad (36)$$

This result coincides, after Wick rotation, with the standard value for the squared Debye screening mass (cf. [14, 23])

$$m_D^2 = \frac{2}{3}g^2T^2, \quad (37)$$

while the result of Eq. (34) implies an imaginary value for the screening mass.

Appearance of anti-screening apparently invalidates the perturbative approach which led to this result. On the other hand, the procedure that reproduces screening with the standard value of  $m_D$  does not provide a viable alternative either. It is based on a singular charged gluon propagator. Source of these singularities is the change in symmetry which in turn enforces a change in the number of zero modes of the associated differential operators. While only one zero mode corresponding to the covariant derivative  $D_3$  exists at fixed  $x_\perp$ , the spectrum of the ordinary derivative  $\partial_3$  of the  $U(1)^3$  theory at  $g = 0$  contains three zero-modes. The difficulties encountered when treating the Polyakov loop variables as Gaussian variables are not specific to our particular approach. As is well known, when employing in finite temperature perturbation theory the temporal gauge  $A_0 = 0$ , “spurious” double poles appear which have to be eliminated by additional prescriptions (cf. [24], [25], [26]). Here, the origin of the difficulties, is actually the elimination of physical variables, the Polyakov loop variables or, in the  $g = 0$  limit, the  $N^2 - 1$  transverse photons. Even after implementation of prescriptions for handling singularities, the resulting formalism remains defective. Most importantly in the course of these manipulations, a QED like shift symmetry ( $Z$ ) associated with the Polyakov loop variables  $a_3$  has been introduced which is not present in the original theory. Thus one cannot resolve the problems by resorting to ambiguous or incomplete gauge fixing procedures. Rather the presence of anti-screening must be interpreted as a dynamical failure of perturbation theory indicating instability of the perturbative vacuum. In the following section we shall show that the vacuum of Polyakov loops is that of ultralocal rather than of Gaussian variables. Perturbation theory built upon this modified vacuum will turn out to be free of the above infrared problems.

### 3 Dynamics of Polyakov loops

### 3.1 Ultralocal Polyakov Loops

In this section we shall explicitly account for the non-Gaussian nature of the Polyakov loop variables  $a_3(x_\perp)$  and respect the finite limit of integration associated with these variables. To this end we first consider the Polyakov loop dynamics in the absence of coupling to the other degrees of freedom. The corresponding generating functional is, in the Euclidean, given by

$$\begin{aligned} Z_0 &= \int d[a_3] \Delta_{\text{FP}}[a_3] \exp \left\{ -1/2 \int d^4x (\partial_\mu a_3(x_\perp))^2 \right\} \\ &= \int_{-\pi/2}^{\pi/2} \prod_{x_\perp} d\tilde{a}_3(x_\perp) \cos^2 \tilde{a}_3(x_\perp) \exp \left\{ -\frac{2\ell}{g^2 L} \sum_{y_\perp, \delta_\perp} (\tilde{a}_3(y_\perp + \delta_\perp) - \tilde{a}_3(y_\perp))^2 \right\}. \end{aligned} \quad (38)$$

We have discretized transverse space time, introduced the lattice spacing  $\ell$ , lattice unit vectors  $\delta_\perp$  and have rescaled the Polyakov loop variables

$$\tilde{a}_3(x_\perp) = gLa_3(x_\perp)/2.$$

In the continuum limit,

$$\frac{\ell}{g^2 L} \sim \frac{\ell}{L} \frac{1}{\ln \frac{\ell}{L}} \rightarrow 0, \quad (39)$$

and therefore the nearest neighbour interaction generated by the Abelian field energy of the Polyakov loop variables is negligible. As a consequence, in the absence of coupling to other degrees of freedom, Polyakov loops do not propagate,

$$\langle \Omega | T(a_3(x_\perp) a_3(0)) | \Omega \rangle \sim \left( \frac{\ell}{g^2 L} \right)^{x_\perp/\ell} \rightarrow \delta^3(x_\perp). \quad (40)$$

Although the above procedure is similar to the strong coupling limit in lattice gauge theory, here we have not invoked a strong coupling approximation. In the lattice dynamics of single links, the factor  $1/g^2$  appears in the action and, as a consequence, continuum limit and strong coupling limit describe two different regimes of the lattice theory. In the Polyakov loop dynamics on the other hand which is controlled by the factor  $\frac{\ell}{g^2 L}$ , strong coupling and continuum limit coincide.

Non-flat measures for the Polyakov loop variables with corresponding limited ranges of integration appear in gauge fixed formulations of QCD irrespective of space-time dimension and are also important for the structure of the lower dimensional gauge fixed theories. For 1+1 dimensional QCD with adjoint fermions e.g. it has been shown [27] that only by accounting properly for the non-flatness of the measure the symmetries of the system are correctly described. However the specific dynamical consequences of the compactness of these variables depend in general on the dimension of space-time. It is interesting that the property of ultralocality of the Polyakov loop variables seems to be unique for 3+1 dimensions. As dimensional arguments dictate, the relevant factor controlling the size of the action (cf. Eq. (38)) is  $\frac{1}{g^2 L}$  in 2+1 dimensions, implying non-trivial dynamics of the Polyakov loop variables  $a_3$ , and becomes  $\frac{1}{g^2 \ell L}$  in 1+1 dimensions which exhibits the characteristic dependence on the time slice of quantum mechanical variables. Furthermore

we remark that the above result is a consequence of the finite range of integration of the Polyakov loop variables. If we extend the range of definition to the full real axis, the functional

$$Z_0^{\text{QED}} = \int_{-\infty}^{\infty} \prod_{x_{\perp}} d\tilde{a}_3(x_{\perp}) \cos^2(\tilde{a}_3(x_{\perp})) \exp \left\{ -\frac{2\ell}{g^2 L} \sum_{y_{\perp}, \delta_{\perp}} (\tilde{a}_3(y_{\perp} + \delta_{\perp}) - \tilde{a}_3(y_{\perp}))^2 \right\} \quad (41)$$

generates the ordinary Green functions of photons propagating in the 1-2 plane with polarization in the 3 direction (as shown above, after extending the range of  $a_3$  the presence of the Faddeev–Popov determinant is irrelevant).

The ultralocality of the Polyakov loop variables is the basis of the further developments and allows us to disregard the Abelian contribution of  $a_3$  to the action. We accordingly rewrite the generating functional of Eq. (19) as

$$Z = \int d[\psi, \bar{\psi}] \prod_{\mu=0}^2 d[A_{\mu}] \exp \left\{ i(S[A_{\perp}, \psi, \bar{\psi}] + S_{gf}[A_{\perp}^3]) \right\} \\ \cdot \int d[a_3] \Delta_{\text{FP}}[a_3] \exp \left\{ i \int d^3 x_{\perp} [g a_3(x_{\perp}) u(x_{\perp}) + g^2 a_3^2(x_{\perp}) v(x_{\perp})] \right\} . \quad (42)$$

The composite field  $u(x_{\perp})$  is generated by the 3 gluon interaction and the interaction of the Polyakov loops with quarks,

$$u(x_{\perp}) = \int_0^L dx_3 \left\{ i \Phi_{\mu}^{\dagger}(x) \overleftrightarrow{\partial}_3 \Phi^{\mu}(x) - \bar{\psi}(x) \frac{\tau_3}{2} \gamma_3 \psi(x) \right\} , \quad (43)$$

while the field  $v(x_{\perp})$  is generated by the 4 gluon interaction,

$$v(x_{\perp}) = \int_0^L dx_3 \Phi_{\mu}^{\dagger}(x) \Phi^{\mu}(x) . \quad (44)$$

Eq. (42) is the essential result of this section and can serve on the one hand as starting point for development of a Ginzburg–Landau theory for the order parameter  $a_3$  of the confinement-deconfinement transition. In this case one has to formally integrate out the other degrees of freedom. On the other hand, one may integrate out the Polyakov loop variables  $a_3$ . Here, we shall choose this alternative option and investigate further the consequences of the peculiar property of ultralocality of the Polyakov loop variables.

### 3.2 Effective Action and Order Parameter

In this section we integrate out explicitly the Polyakov loop variables and derive the generating functional for gluon ( $A_{\mu}$ ,  $\mu = 0, 1, 2$ ) and quark Green functions; in this way we also will be able to arrive at a novel representation of the Polyakov loop expectation value and the associated correlation function. To this end we expand the exponential in Eq. (41) and keep only the leading term in a  $\ell/(g^2 L)$  expansion,

$$\int d[a_3] \Delta_{\text{FP}}[a_3] \exp \left\{ i \int d^3 x_{\perp} [g a_3(x_{\perp}) u(x_{\perp}) + g^2 a_3^2(x_{\perp}) v(x_{\perp})] \right\} \\ \approx \prod_{\vec{x}_{\perp}} \left[ 1 + i \frac{\ell^3}{L^2} \left( \frac{\pi^2}{3} - 2 \right) v(\vec{x}_{\perp}) \right] . \quad (45)$$

This expansion is justified if the fluctuations of the gluon fields are controlled by the ultraviolet cutoff  $1/\ell$  as in a non-interacting theory, and if a possible violation of the reflection symmetry ( $x_3 \rightarrow -x_3$ ) is limited to finite momenta ( $|p_{3,n}| < \Lambda \ll \frac{1}{\ell}$ ),

$$A_\mu \sim \frac{1}{\ell} \quad \text{i.e.} \quad v \sim \frac{L}{\ell^2}, \quad u \sim \frac{\Lambda L}{\ell^2}.$$

We also note that in this expansion, we disregard non-perturbative dynamics associated with singular field configurations. We thus rewrite the generating functional as

$$Z = \int d[A, \psi, \bar{\psi}] e^{iS_{\text{eff}}[A, \psi, \bar{\psi}]} \quad (46)$$

with the effective action given by

$$S_{\text{eff}}[A, \psi, \bar{\psi}] = \int d^4x \mathcal{L}_{\text{eff}} = S[A, \psi, \bar{\psi}] + S_{\text{gf}}[A_\perp^3] + \frac{1}{2} M^2 \sum_{a=1,2} \int d^4x A_\mu^a(x) A^{a,\mu}(x). \quad (47)$$

Expectation values and correlation functions of the Polyakov loops are calculated correspondingly with the following results,

$$\begin{aligned} \langle \Omega | \sin(gLa_3(x_\perp)/2) | \Omega \rangle &\approx \frac{1}{Z[0]} \frac{16i\ell^3}{9\pi L} \int d[A, \psi, \bar{\psi}] u(x_\perp) e^{iS_{\text{eff}}[A, \psi, \bar{\psi}]} \\ &\sim \langle \Omega | u(x_\perp) | \Omega \rangle, \end{aligned} \quad (48)$$

$$\langle \Omega | T(\sin(gLa_3(x_\perp)/2) \sin(gLa_3(y_\perp)/2)) | \Omega \rangle \sim \langle \Omega | T[u(x_\perp) u(y_\perp)] | \Omega \rangle. \quad (49)$$

The effective action of QCD after integrating out the Polyakov loops (Eq. (47)) is that of QCD in the naive axial gauge ( $A_3 = 0$ ) complemented by a lower dimensional residual gauge fixing term, a mass term and the already discussed change in boundary conditions of charged gluon and quark fields. In the spirit of the Abelian projection we write the effective Lagrangian as

$$\begin{aligned} \mathcal{L}_{\text{eff}} &= -\frac{1}{2} (d_\mu^* \Phi_\nu^\dagger - d_\nu^* \Phi_\mu^\dagger) (d^\mu \Phi^\nu - d^\nu \Phi^\mu) - \partial_3 \Phi_\mu^\dagger \partial^3 \Phi^\mu + M^2 \Phi_\mu^\dagger \Phi^\mu \\ &\quad - \frac{1}{4} f_{\mu\nu} f^{\mu\nu} - \frac{1}{2} \partial_3 A_\mu \partial^3 A^\mu - \frac{1}{2\xi} \left( \frac{1}{L} \int_0^L dx_3 \partial^\mu A_\mu \right)^2 \\ &\quad + ig f^{\mu\nu} \Phi_\mu^\dagger \Phi_\nu - \frac{g^2}{4} (\Phi_\mu^\dagger \Phi_\nu - \Phi_\nu^\dagger \Phi_\mu) (\Phi^{\nu\dagger} \Phi^\mu - \Phi^{\mu\dagger} \Phi^\nu) \\ &\quad + \bar{\psi} (i\not{d} - m) \psi + \bar{\psi} i\gamma^3 \partial_3 \psi - \frac{g}{\sqrt{2}} \bar{\psi} \gamma^\mu (\Phi_\mu \tau_+ + \Phi_\mu^\dagger \tau_-) \psi. \end{aligned} \quad (50)$$

In addition to the charged gluon fields we have introduced Abelian field strengths generated by the neutral gluons,

$$f_{\mu\nu} = \partial_\mu A_\nu - \partial_\nu A_\mu, \quad A_\mu = A_\mu^3, \quad (51)$$

and the corresponding covariant derivatives

$$d_\mu = \partial_\mu + ig A_\mu, \quad \not{d} = \gamma^\mu \left( \partial_\mu + ig A_\mu \frac{\tau_3}{2} \right). \quad (52)$$

The Polyakov loops leave the antiperiodic boundary conditions and the mass term of the charged gluon fields as their signatures. The antiperiodic boundary conditions reflect the mean value of the Polyakov loop variables, the geometrical mass their fluctuations. Clearly the precise value of this geometrical mass

$$M^2 = \left( \frac{\pi^2}{3} - 2 \right) \frac{1}{L^2} \quad (53)$$

depends on the particular form of the Faddeev–Popov determinant. The emergence of this geometrical mass with its characteristic independence of the coupling constant is a consequence of the finite range of integration. Unlike mass generation, the change in boundary conditions is a less common phenomenon. For its interpretation we observe that the transformation to antiperiodic charged gluon variables is a merely formal device. The antiperiodic boundary conditions in (23) actually describe the appearance of Aharonov–Bohm fluxes in the elimination of the Polyakov loop variables. Periodic charged gluon fields may be used if the differential operator  $\partial_3$  is replaced by

$$\partial_3 \rightarrow \partial_3 + \frac{i\pi}{2L}[\tau_3, \quad . \quad (54)$$

As for a quantum mechanical particle on a circle, such a magnetic flux is technically most easily accounted for by an appropriate change in boundary conditions — without changing the original periodicity requirements. With regard to the rather unexpected physical consequences, the space-time independence of this flux is important, since it induces global changes in the theory. These global changes are missed if the Polyakov loops are treated as Gaussian variables. Thus expressed in these more physical terms, the charged gluons are massive and move in a constant color neutral gauge field pointing in the spatial 3 direction of the strength  $\frac{\pi}{gL}$ . Since  $x_3$  is a compact variable we can associate a color magnetic flux with this gauge field,

$$\Phi_{\text{mag}} = \frac{\pi}{g} . \quad (55)$$

The corresponding magnetic field of strength

$$B = \frac{1}{gL^2} \quad (56)$$

lives however in the unphysical embedding space — e.g. in the interior of the cylinder whose surface is the spatial manifold of  $\text{QCD}_{2+1}$ .

Summarizing the results of this section, we emphasize the crucial property of ultralocality of the Polyakov loops. It implies that these variables do not constitute physical degrees of freedom; rather they are dependent variables. In the axial gauge these dependent variables are composite gluon fields. Propagation of the Polyakov loops occurs only via intermediate excitation of “two gluon states” created by the operator  $u(x_\perp)$ . In the course of integrating out these dependent variables, dynamical differences between neutral and charged gluons arise. Charged gluons acquire a mass and are subject to antiperiodic boundary conditions while neutral gluons remain unaffected at the perturbative level.

It appears that with these dynamical differences, the formalism contains the seeds for Abelian dominance of long distance physics. Results of recent lattice calculations of the gluon propagator in maximally Abelian gauge have actually been interpreted in terms of massive charged and essentially massless neutral gluons [28].

### 3.3 Phases of QCD in Axial Gauge

The following discussion will focus on the properties of the SU(2) Yang Mills theory. If dynamical quarks are present, the charge conjugation (Eq. (25)) is not a symmetry transformation of the system. Formally, the Lagrangian of Eq. (50) remains invariant if the quark fields too are transformed,

$$\psi \rightarrow \tau_1 \psi . \quad (57)$$

This transformation changes however the boundary conditions (Eq. (23)). In the absence of dynamical quarks, the auxiliary field  $u(x_\perp)$  which is odd under charge conjugation

$$C : \quad u(x_\perp) \rightarrow -u(x_\perp) \quad (58)$$

serves, after elimination of the Polyakov loop variables, as an order parameter for the realization of charge conjugation symmetry. In the confined phase, charge conjugation is realized

$$\langle 0|u(x_\perp)|0\rangle = 0 \quad , \quad L > L_c \quad (59)$$

and spontaneously broken in the deconfined phase

$$\langle 0|u(x_\perp)|0\rangle \neq 0 \quad , \quad L < L_c . \quad (60)$$

The deconfinement transition occurring when decreasing  $L$  beyond the critical value is accompanied or possibly generated by color currents in the compact 3-direction. The presence of these currents signals a simultaneous breakdown of the reflection symmetry  $x_3 \rightarrow -x_3$  as implied by the non-vanishing vacuum expectation value of  $u$ .

The perturbative ground state of QCD is symmetric under charge conjugation, i.e., it respects the center symmetry. This is the distinctive property of QCD in the (modified) axial gauge. Unlike ‘‘perturbative’’ gauge choices such as covariant gauges or the Coulomb gauge in the standard treatment which incorporate the symmetries of electrodynamics (the  $U(1)^{N^2-1}$  theory), the modified axial gauge with its non-perturbative resolution of Gauss’ law preserves the  $Z_N$  symmetry characteristic for Yang Mills theory. By respecting the charge symmetry, the perturbative vacuum satisfies the confinement criterium and indicates an infinite energy to be associated with a static fundamental charge. Needless to say, the perturbative limit is insufficient to describe realistically the phenomena related to confinement; it however appears that certain global properties of the system are properly accounted for already at this (modified) perturbative level, leading naturally into the confined phase of QCD.

The correlation function corresponding to this auxiliary field provides further characterization of the phases of QCD. After rotation to Euclidean time

$$x_0 \rightarrow -ix_0^E \quad (61)$$

the correlation function of the Polyakov loops yields the interaction energy  $V$  of static color charges (in the fundamental representation). Thus we have after adjusting an additive constant in  $V$  which accounts for the proportionality factor in Eq. (49)

$$\exp\{-LV(r)\} = \langle \Omega | T [u(x_{\perp}^E) u(0)] | \Omega \rangle = \mathcal{D}(r), \quad r^2 = (x^E)^2. \quad (62)$$

Due to the rotational invariance in Euclidean transverse space, we are free to choose  $x^E$  to point in the time direction. We insert a complete set of excited states

$$\exp\{-LV(r)\} = \sum_n |\langle n | u(0) | \Omega \rangle|^2 e^{-E_n r}. \quad (63)$$

In the confined phase, the ground state does not contribute to this sum (cf. Eq. (59)). If the spectrum exhibits a gap, the potential energy  $V$  increases linearly with  $r$  for large separations,

$$V(r) \approx \frac{E_1}{L} r \quad \text{for } r \rightarrow \infty \quad \text{and } L > L_c. \quad (64)$$

Since on the other hand, the slope is given by the string tension  $\sigma$ , we conclude that the spectrum of states excited by the composite operator  $u$  possesses a gap which increases linearly with the extension  $L$ . Thus in Yang Mills theory at finite extension the phenomenon of confinement is connected to a shift in the spectrum of gluonic excitations to excitation energies

$$E \geq \sigma L. \quad (65)$$

Note that the class of states excited by the Polyakov loop variables are associated in QED with a vanishing threshold energy. This result implies in particular that in the confined phase, glueball states which, for sufficiently large values of  $L$ , should not be affected by the finite extension, cannot be excited by  $u$ . The characteristic property of the “two gluon” operator  $u$  which most likely is responsible for this confinement phenomenon is the negative  $C$ -parity. It is remarkable that perturbation theory yields the linear rise of the static quark-antiquark potential at large separations. The charge symmetric ground state does not contribute to the sum in Eq. (63), and the spectrum of charged gluons exhibits a gap as a consequence of the antiperiodic boundary conditions and the geometrical mass term. The resulting  $L$ -dependence of the perturbative string tension

$$\sigma_{\text{pert}} = \frac{2}{L} \sqrt{M^2 + (\pi/L)^2} \quad (66)$$

is, at this point, determined by dimensional arguments and obviously not realistic.

A further characterization of the negative and positive  $C$ -parity sectors of the  $Z_2$  symmetric phase can be obtained through a discussion of the adjoint Polyakov loops. The adjoint Polyakov loop is defined with the matrices  $T^a$  of the adjoint representation as

$$\mathcal{P}_{\text{ad}}(x_{\perp}) = \frac{1}{3} \text{Tr P exp} \left( ig \int_0^L dz A_3^a(x_{\perp}, z) T^a \right) \quad (67)$$

and, if expressed in terms of the variables  $a_3$  of Eq. (17), given by

$$\mathcal{P}_{\text{ad}}(x_{\perp}) = \frac{1}{3} (1 - 2 \cos gLa_3(x_{\perp})) . \quad (68)$$

Functional integration over the ultralocal Polyakov loop variables is performed as in Sect. 3.2 (cf. Eqs. (47) – (49)) and yields expressions of expectation value and associated correlator of the adjoint Polyakov loop in terms of the composite field  $v(x_\perp)$  of Eq. (44)

$$\langle \Omega | \mathcal{P}_{\text{ad}} | \Omega \rangle \sim \langle \Omega | v | \Omega \rangle, \quad \langle \Omega | T [\mathcal{P}_{\text{ad}}(x_\perp) \mathcal{P}_{\text{ad}}(0)] | \Omega \rangle \sim \langle \Omega | T [v(x_\perp)v(0)] | \Omega \rangle. \quad (69)$$

Unlike the order parameter  $u(x_\perp)$ , the field  $v(x_\perp)$  has positive  $C$ -parity and is therefore not prevented by a selection rule from acquiring an expectation value. Indeed already at the perturbative level such an expectation value occurs, given by the tadpole contribution to the  $a_3$  effective action generated by the corresponding 4-gluon vertex. As a consequence of the non-vanishing expectation value, the interaction energy between static adjoint charges

$$\exp \{-LV_{\text{ad}}(r)\} = \sum_n |\langle n | v(0) | \Omega \rangle|^2 e^{-E_n r} \quad (70)$$

decreases exponentially at large distances,

$$V_{\text{ad}}(r) \sim \frac{1}{r^2} e^{-E_1 r}, \quad (71)$$

with  $E_1$  the threshold of excited states. On the other hand, we expect quite generally this exponential decrease to be determined by the lowest glueball mass. Thus, unlike the two gluon operator  $u(x_\perp)$ , the composite operator  $v(x_\perp)$  yields excitations in the physical sector of hadronic states.

### 3.4 Confinement-Deconfinement Transition

The perturbative  $Z_2$  symmetric phase of QCD reached in this modified axial gauge not only shares characteristic properties with the non-perturbative confining phase, it also exhibits signatures which point to the necessity of a phase transition to the deconfined phase with the  $Z_2$  symmetry spontaneously broken. We start with a discussion of the ground state energy density. The total energy of the system is given by

$$E = L_\perp^2 \int \frac{d^2 k}{(2\pi)^2} \sum_{n=-\infty}^{\infty} \left[ \left( k^2 + \frac{\pi^2}{L^2} (2n)^2 \right)^{1/2} + 2 \left( k^2 + M^2 + \frac{\pi^2}{L^2} (2n+1)^2 \right)^{1/2} \right], \quad (72)$$

with  $L_\perp$  denoting the extension of the system in the transverse (1,2) directions. The two terms represent the zero point energies of neutral and charged gluons, respectively. For technical simplicity of this qualitative discussion we shall neglect the charged gluon mass and compute the ground state energy with the help of dimensional regularization. It is straightforward to show

$$\mu^{2-2\omega} \int \frac{d^{2\omega} k}{(2\pi)^{2\omega}} \sum_{n=-\infty}^{\infty} \left( k^2 + \frac{1}{L^2} (2\pi n + \chi)^2 \right)^{1/2} = -\frac{\pi^2}{45L^3} \left[ 1 - \frac{15}{8} \left( \left( \frac{\chi}{\pi} - 1 \right)^2 - 1 \right)^2 \right] \quad (73)$$

in the limit  $\omega \rightarrow 1$ . This result implies the standard Casimir energy or Stefan Boltzmann law for the neutral gluons ( $\chi = 0$ )

$$E_{\text{neut}}/(L_{\perp}^2 L) = -\frac{\pi^2}{45L^4} \quad (74)$$

while (up to an important sign) the expression for the charged gluon energy ( $\chi = \pi$ ) is reminiscent of the fermionic contribution to the energy density

$$E_{\text{ch}}/(L_{\perp}^2 L) = \frac{7}{4} \frac{\pi^2}{45L^4} . \quad (75)$$

The total ground state energy is thus given by

$$E_{\text{ch}}/(L_{\perp}^2 L) = \frac{3}{4} \frac{\pi^2}{45L^4} . \quad (76)$$

Due to the antiperiodic boundary conditions of the charged gluons a change of sign occurs in the ground state energy which, in turn, implies a change of sign in the pressure, i.e., a repulsive Casimir force acting between the plates enclosing the system. Invoking covariance, this change in the characteristic properties of the Casimir effect is seen to lead to a change of sign in the relevant thermodynamic properties of the same system at infinite extension but finite temperature. Thus the perturbative  $Z_2$  phase is thermodynamically unstable. This instability is of little relevance for the large extension or low temperature phase, where the non-perturbative phenomena of confinement and generation of a mass gap in the “hadronic” sector will change the power law in the Casimir energy and pressure into an exponential dependence. Likewise, the appearance of the imaginary “screening mass” in the polarization propagator discussed above (cf. Eq. (34)) which signals this instability poses no problems given the zero-range of the Polyakov loop propagator (see below for a more detailed discussion). At small extension or high temperature on the other hand, where a perturbative approach should be appropriate, this instability seems to rule out a  $Z_2$  symmetric high temperature phase. Such a phase indeed would have properties very different from the high temperature phase as deduced from lattice gauge calculations. Trivially, with the center symmetry realized, such a phase would have to exhibit certain characteristics of confinement. Furthermore, irrespective of the dynamics, at high temperatures dimensional reduction should take place. Like quarks in QCD, the charged gluons decouple from the low-lying excitations due to their antiperiodic boundary conditions in the process of dimensional reduction. Thus at small extension or high temperature, the  $Z_2$  symmetric phase is described by  $\text{QED}_{2+1}$  rather than by  $\text{QCD}_{2+1}$ .

From our discussion the following qualitative, axial gauge description of the confinement-deconfinement transition emerges. After a gradual decrease in the threshold of states with negative  $C$ -parity with decreasing  $L$ , the whole spectrum of excitations ( $C = \pm 1$ ) becomes suddenly available when at the deconfinement transition with the breakdown of  $C$ -parity simultaneously string tension (threshold of the  $C = -1$  states) and mass gap in the hadronic sector (threshold of  $C = 1$  states) vanish. In this transition, the charged gluon fields effectively must become periodic (up to possible interaction effects), i.e., the Aharonov–Bohm fluxes (Eq. (55)) are shielded and simultaneously the geometrical mass

$M$  (Eq. (53)) disappears. As a result of the phase transition, the unlimited increase in the lowest single gluon energy

$$\epsilon(\vec{k}_\perp, n_3)^2 = k_\perp^2 + \frac{1}{L^2} \left( \pi^2 (2n_3 + 1)^2 + \left( \pi^2/3 - 2 \right) \right). \quad (77)$$

with decreasing extension  $L$  is prevented and thereby, in dimensional reduction, the correct high temperature limit is reached. In this change of boundary conditions, the degeneracy of oppositely charged gluons with momenta  $n_3 = 0$  and  $n_3 = -1$  is lifted and currents in the 3-direction (cf. Eqs. (43), (60)) are generated. Finally, this change of boundary conditions results in a change in Casimir energy density and pressure which according to Eq. (73) is given by

$$\Delta\epsilon = -\pi^2/12L^4, \quad \Delta p = 3\Delta\epsilon. \quad (78)$$

This estimate is of the order of magnitude of the change in the energy density across the confinement-deconfinement transition when compressing the system,

$$\Delta\epsilon = -0.45/L^4, \quad (79)$$

deduced from the finite temperature lattice calculation of Ref. [29].

In summary, the thermodynamic instability of the  $Z_2$  symmetric perturbative phase implies the presence of non-perturbative phenomena to stabilize this phase and a transition to a phase with broken  $Z_2$  symmetry. If QCD in the high temperature (or small extension) deconfined phase is to be described perturbatively, one therefore has to abandon this modified axial or temporal gauge with its characteristic  $N - 1$  Polyakov loops as zero modes. Starting point has to be QCD at  $g = 0$ , and for this  $U(1)^{N^2-1}$  theory an axial gauge with  $N^2 - 1$  photons as zero modes is more appropriate. This procedure breaks the center symmetry and the Stefan-Boltzmann law at high temperatures is guaranteed by gauge choice.

## 4 Perturbation Theory in the $Z_2$ Symmetric Phase

### 4.1 Feynman Rules

In this section we shall continue our analysis of the  $Z_2$  symmetric phase with a discussion of specific issues in perturbation theory. In this context the perturbative treatment of the Polyakov loop correlator will be of particular importance. The Feynman rules are easily derived from the quadratic part of the effective Lagrangian of Eq. (50). As a result of integrating out the Polyakov loop variables, charged and neutral gluon propagators have different momentum dependences. The charged gluon propagator is given by

$$D_{\mu\nu}^{ab}(p, p_3) = \frac{\delta^{ab}(1 - \delta^{a3})}{p^2 - p_3^2 - M^2 + i\epsilon} \left[ -g_{\mu\nu} + \frac{p_\mu p_\nu}{p_3^2 + M^2} \right] \quad (80)$$

with  $p_3$  derived from antiperiodic boundary conditions,

$$p_3 = \frac{2\pi}{L} \left( n + \frac{1}{2} \right), \quad (81)$$

and the neutral gluon propagator by

$$D_{\mu\nu}^{ab}(p, p_3) = \frac{\delta^{ab}\delta^{a3}}{p^2 - p_3^2 + i\epsilon} \left[ -g_{\mu\nu} + p_\mu p_\nu \left( (1 - \delta_{p_3,0}) \frac{1}{p_3^2} + \delta_{p_3,0} (1 - \xi) \frac{1}{p^2 + i\epsilon} \right) \right] \quad (82)$$

with  $p_3$  derived from periodic boundary conditions,

$$p_3 = \frac{2\pi n}{L} . \quad (83)$$

In the actual calculations, the parameter  $\xi$  of the residual covariant gauge will be set equal to 1 (2+1 dimensional Feynman gauge). The 3- and 4-gluon vertices are standard, except that only three polarizations (0,1,2) appear, and given by

$$V_{\lambda\mu\nu}^{abc}(p, q, r) = g\epsilon^{abc} [(r - q)_\lambda g_{\mu\nu} + (q - p)_\nu g_{\lambda\mu} + (p - r)_\mu g_{\nu\lambda}] \delta^{(3)}(p+q+r) \delta_{p_3+q_3+r_3,0} \quad (84)$$

$$\begin{aligned} W_{\lambda\mu\nu\rho}^{abcd}(p, q, r, s) = & -ig^2 \left[ \epsilon^{fab}\epsilon^{fbc} (g_{\lambda\nu}g_{\mu\rho} - g_{\lambda\rho}g_{\mu\nu}) + \epsilon^{fcb}\epsilon^{fad} (g_{\lambda\nu}g_{\mu\rho} - g_{\lambda\mu}g_{\nu\rho}) \right. \\ & \left. + \epsilon^{fac}\epsilon^{fbd} (g_{\lambda\mu}g_{\nu\rho} - g_{\lambda\rho}g_{\mu\nu}) \right] \delta^{(3)}(p+q+r+s) \delta_{p_3+q_3+r_3+s_3,0} \quad (85) \end{aligned}$$

with  $a, \lambda, p$  etc. denoting color, polarization and momentum of incoming gluons. Finally, the coupling of a Polyakov loop to two gluons has the form

$$V_{\text{ggP}} = V_{3\mu\nu}^{3bc}(p_\perp, q, r) = g\epsilon^{3bc} (r - q)_3 g_{\mu\nu} \delta^{(3)}(p+q+r) \delta_{q_3+r_3,0} . \quad (86)$$

We observe that both neutral and charged gluon propagators are well defined in the infrared. By properly accounting for the zero modes of the differential operators appearing in the quadratic part of the action no infrared infinities are encountered. The antiperiodic boundary conditions and the geometrical mass term yield a well defined charged gluon propagator while as in QED, the residual gauge fixing is instrumental for the proper infrared behavior of the neutral gluon propagator. Thus the characteristic difficulties of the continuum axial gauge propagator, such as the appearance of spurious double poles [30], are not present. The infrared properties are also significantly different from those obtained in standard finite temperature formulation. In our case, infrared infinities can occur only in loops if they are generated by 4-gluon vertices with vanishing external momenta and if both gluons in the loop are neutral. Thus the infrared properties resemble those of scalar QED and the difficulties encountered in finite temperature perturbation theory for QCD (cf. [31]) can therefore be expected to be alleviated in the  $Z_2$  symmetric phase.

The following discussion will focus on the properties of the Polyakov loop correlation function which in Eq. (49) has been expressed in terms of the composite operators  $u(x_\perp)$ . As is well known, this correlation function is, for imaginary times, determined by the free (interaction) energy  $V$  of a static quark-antiquark pair at temperature  $T = 1/L$  (cf. Eq. (62)), and therefore allows us to further study important properties of the  $Z_2$  symmetric phase. Furthermore, this discussion will offer the possibility to display within perturbation theory certain characteristics of the modified axial gauge, in particular its high momentum behaviour.

## 4.2 Polyakov Loop Correlator to Order $g^2$

The novel aspects of the following development are related to the ultralocality property of the Polyakov loops. As a consequence of ultralocality, the Polyakov loop correlator is given by a one particle *irreducible* 2-point function, i.e., the vacuum polarization rather than by the one particle *reducible* Green function of standard Gaussian variables. This structural change implies a very different physics content of the relation (62) already at the perturbative level. More precisely, according to the definition of the field  $u$  (Eq. (43)), the correlation function can be identified with the color neutral,  $\mu = \nu = 3$  component of the vacuum polarization tensor  $\Pi^{\mu\nu}$ , evaluated with the external Polyakov loop vertices of Eq. (86). Thus, up to a constant, the interaction energy is related to the vacuum polarization by

$$V(r) = -\frac{1}{L} \ln w(r) \quad (87)$$

with

$$w(r) = \int \frac{d^3 p}{(2\pi)^3} \Pi_{\text{gg}}^{33}(ip_0, p_1, p_2) e^{i\vec{p}\vec{r}} , \quad r \neq 0 . \quad (88)$$

In one loop approximation (Fig. 3)  $\Pi_{\text{gg}}^{33}$  is given by

$$\Pi_{\text{gg}}^{33}(p) = \frac{2g^2}{L} \sum_{q_3} q_3^2 \int \frac{d^3 q}{(2\pi)^3} \sum_{a,b \neq 3} D_{\mu\nu}^{ab}(q, q_3) D^{ab,\mu\nu}(p - q, q_3) . \quad (89)$$

After performing the sum over color and Lorentz indices, the divergent 3-dimensional integration is most conveniently carried out in dimensional regularization with the result

$$\begin{aligned} \Pi_{\text{gg}}^{33}(p) &= \frac{ig^2}{4\pi L} \sum_{q_3} q_3^2 \left[ \left( \frac{p^3}{2(q_3^2 + M^2)^2} - \frac{2p}{q_3^2 + M^2} + \frac{4}{p} \right) \ln \left( \frac{2\sqrt{q_3^2 + M^2} + p}{2\sqrt{q_3^2 + M^2} - p} \right) \right. \\ &\quad \left. - \frac{2p^2}{(q_3^2 + M^2)^{3/2}} \right] e^{-\lambda|q_3|} . \end{aligned} \quad (90)$$

In this regularization procedure, divergencies are encountered only in the final sum over the ‘‘Matsubara momenta’’  $q_3$  which as indicated above we regularize by a heat kernel method. The final expression has to be evaluated numerically. For vanishing momentum, Eq. (90) simplifies to

$$\Pi_{\text{gg}}^{33}(0) = \frac{ig^2}{\pi L} \sum_{q_3} \frac{q_3^2}{\sqrt{q_3^2 + M^2}} e^{-\lambda|q_3|} . \quad (91)$$

The complete vacuum polarization associated with the Polyakov loop variables is obtained by adding the (momentum independent) tadpole contribution

$$\Pi_{\text{tp}}^{33} = \frac{ig^2}{\pi L} \sum_{q_3} \sqrt{q_3^2 + M^2} e^{-\lambda|q_3|} \quad (92)$$

which yields (for  $p = 0$ )

$$\Pi_{\text{gg}}^{33}(0) + \Pi_{\text{tp}}^{33} = \frac{1}{3} \frac{ig^2}{L^2} (1 + \delta\pi) , \quad (93)$$

with

$$\delta\pi = \frac{6L}{\pi} \sum_{q_3} \left[ \frac{q_3^2 + M^2/2}{\sqrt{q_3^2 + M^2}} - |q_3| \right] = 0.024 \quad (94)$$

characterizing the influence of the geometrical mass. As in Eq. (34) the unusual sign for the vacuum polarization is obtained. Unlike for massless Gaussian variables, this sign does not imply a dynamical instability for the ultralocal Polyakov loops.

For large spacelike momenta, the vacuum polarization is given by

$$\begin{aligned} \Pi_{\text{gg}}^{33}(p) \approx & -\frac{ig^2}{4\pi} \left[ (-p^2)^{3/2} L S_1 \right. \\ & \left. - \frac{p^2}{9\pi} \left\{ 33 \left( \ln \frac{\lambda(-p^2)^{1/2}}{2} + \gamma \right) + 1 \right\} + \frac{(-p^2)^{1/2}}{L} S_2 \right] \end{aligned} \quad (95)$$

with the sums

$$\begin{aligned} S_1 &= -\frac{\pi}{2L^2} \sum_{q_3} \frac{q_3^2}{(q_3^2 + M^2)^2} = \frac{-\pi}{16} \left( \frac{\tanh LM/2}{LM/2} + \frac{1}{\cosh^2 LM/2} \right) = -0.32 \\ S_2 &= 2\pi M^2 \sum_{q_3} \frac{1}{q_3^2 + M^2} = \pi LM \tanh \frac{LM}{2} = 1.83 \end{aligned} \quad (96)$$

In the modified axial or temporal gauge, the leading term of the vacuum polarization at large momenta is not of the familiar form  $p^2 \ln p^2$ . Although such a term is present in the expansion, it is subleading to the  $Lp^3$  contribution. The leading asymptotic term is generated by the ‘‘gauge term’’ ( $\sim p^\mu p^\nu / (p_3^2 + M^2)$ ) in the propagator (80) as can be seen from the dependence of the expression (89) on size or inverse temperature  $L$  of the system. Summation over the wave numbers  $q_3$  contributes a factor  $L^{-1}$ , and so does each of the two momenta from the vertices ( $q_3^2$ ). A gauge term in the propagator contributes a factor  $L^2$ . Thus the product of the two gauge terms gives rise to the leading linear dependence on  $L$  which in turn implies the  $p^3$  dependence in Eq. (95).

One might argue that this large momentum behaviour of the vacuum polarization is a gauge artefact. Indeed similar deviations from standard large momentum behavior are also present in QED. In Appendix A, we have sketched the calculation of the one loop fermion self energy at large momenta in a modified axial gauge. The leading term,

$$\Sigma(p) \approx \frac{e^2}{192} \not{p}_\perp L \sqrt{-p_\perp^2}, \quad (97)$$

is generated by the corresponding gauge term in the photon propagator. In this Appendix, it is also shown that gauge terms do not contribute to gauge invariant quantities such as the two point function

$$\langle 0 | T(\bar{\psi}_\beta(y) \exp \left\{ -ie \int_x^y ds^\mu A_\mu \right\} \psi_\alpha(x)) | 0 \rangle$$

obtained by insertion of a gauge string into the definition of the fermion propagator. In QCD this alternative does not exist. The Polyakov loop correlator is (before gauge

fixing) a gauge invariant quantity. Unlike in QED where, in the process of gauge fixing, the fermion field operators are made gauge invariant by attaching gauge strings which extend over the whole compact direction, the appearance of the extension  $L$  in the leading term of Eq. (96) is due to the intrinsic property of the Polyakov loops of winding around the compact direction and is not generated by the gauge choice.

The complete momentum dependence of the vacuum polarization (tadpole included) associated with the Polyakov loops can be evaluated numerically with the help of Eq. (90) and Appendix B. The physics content of the Polyakov loop correlator is exhibited by the following discussion of the static quark-antiquark interaction energy (Eqs. (87), (88)). Instead of performing directly the Fourier transform of  $\Pi_{\text{gg}}^{33}$  (cf. Eq. (88)), it is more convenient to transform the Euclidean gluon propagator to  $r$ -space,

$$w(r) = \frac{4g^2}{L} \sum_{q_3} q_3^2 \tilde{D}_{\mu\nu}(r, q_3) \tilde{D}_{\mu\nu}(r, q_3) \quad (98)$$

with

$$\tilde{D}_{\mu\nu}(r, q_3) = \left[ \delta_{\mu\nu} - \frac{1}{\omega_3^2} \partial_\mu \partial_\nu \right] \frac{1}{4\pi r} e^{-\omega_3 r} \quad (99)$$

and

$$\omega_3 = \sqrt{q_3^2 + M^2} . \quad (100)$$

Performing the differentiations and summations over Lorentz indices, we obtain the sum

$$w(r) = \frac{g^2}{2\pi^2 L r^6} \sum_{q_3} \frac{q_3^2 e^{-2\omega_3 r}}{\omega_3^4} \left( 3 + 6(\omega_3 r) + 5(\omega_3 r)^2 + 2(\omega_3 r)^3 + (\omega_3 r)^4 \right) \quad (101)$$

which can only be evaluated numerically for general  $r$ . Taking the logarithm of Eq. (101), we see that the  $r$ -dependent part of the potential does not contain  $g^2$  anymore, i.e., it is purely “kinematical” at one loop order. For small separations a logarithmic potential is obtained

$$V(r) \approx \frac{6}{L} \ln(\mu r) + \text{O}(1) , \quad r/L \ll 1 \quad (102)$$

( $\mu$  is an arbitrary scale). The leading  $1/r^6$  term in this small distance expansion of  $w$  is the Fourier transform of the leading term  $L(-p^2)^{3/2}$  in  $\Pi_{\text{gg}}^{33}$  for large spacelike momenta, and is therefore generated from the gauge terms. This will be seen to be true also in higher order. For large separations the potential of static charges increases linearly with the separation. The dominant contribution to the sum (96) comes from the lowest Matsubara momenta ( $n = 0, -1$ ) and we find

$$V(r) \approx \sigma_{\text{pert}} r + \frac{2}{L} \ln(\mu r) + \text{O}(1) , \quad r/L \gg 1 . \quad (103)$$

Here the leading contribution is determined by the singularity of the vacuum polarization  $\Pi_{\text{gg}}^{33}(p)$  closest to the real axis. The exponential fall-off and therefore the perturbative “string tension” (cf. Eq. (66)) is determined by the threshold energy  $2\omega_3|_{n=0}$  for producing two charged gluons. We also note that for infinite extension or zero temperature, the interaction energy vanishes to this order. As in other evaluations of the interaction

energy, this has to be interpreted as arising from the cancellation between singlet and triplet contributions to the free energy. In this way the free energy actually becomes the color averaged interaction energy which vanishes to lowest order. This degeneracy does however not persist at finite extension or temperature where for instance neutral and charged gluons are distinguished by geometrical mass term and boundary conditions. This distinction disappears for large  $L$ ; however, it is independent of the coupling constant and thus gives rise to this “kinematical” one loop result. Finally, we stress once more that due to the ultralocality of the Polyakov loop variables, the “wrong” sign of  $\Pi^{33}(0)$  does not give rise to an unphysical behaviour of the static quark interaction energy at large distances.

### 4.3 Gluon Two-Point Function to One Loop

In this section, we continue to develop perturbation theory in the modified axial gauge. We will evaluate the gluon two-point function to order  $g^2$  and thereby address issues of regularization and renormalization. A topic of special importance will be the asymptotic behaviour of the gluon propagator at large momenta.

For both the technical evaluation as well as for the physics interpretation it is advantageous to separate the  $g_{\mu\nu}$  and the  $p_\mu p_\nu$  contributions to the gluon propagator  $D_{\mu\nu}^{ab}(p)$ , Eqs. (80), (82). We first evaluate the vacuum polarization insertion into the charged gluon propagator, Fig. 4a. The formal expression for this insertion is

$$\Pi_{\text{gg}}^{\mu\nu}(p, p_3) = \frac{g^2}{L} \sum_{q_3} \int \frac{d^3 q}{(2\pi)^3} \frac{N_0^{\mu\nu} + N_1^{\mu\nu} + N_2^{\mu\nu}}{(q^2 - q_3^2 - M^2 + i\epsilon)((q-p)^2 - (q_3 - p_3)^2 + i\epsilon)} \quad (104)$$

The choice of the momenta is indicated in Fig. 4a. The loop momentum  $(q, q_3)$  denotes the charged gluon momentum. According to the separation of the propagators into the  $g_{\mu\nu}$  and the gauge term (cf. Eqs. (80), (82)), the vacuum polarization has been broken up into contributions arising from none, one or two gauge terms

$$\begin{aligned} N_0^{\mu\nu} &= g^{\mu\nu}(2q^2 + 5p^2 - 2qp) - 3p^\mu p^\nu + 6q^\mu q^\nu - 3(p^\mu q^\nu + q^\mu p^\nu) , \\ N_1^{\mu\nu} &= \frac{1 - \delta_{q_3, p_3}}{(q_3 - p_3)^2} \left[ -g^{\mu\nu}(q^2 - p^2)^2 + p^\mu p^\nu(p^2 - 2q^2) + q^\mu q^\nu(q^2 - 2p^2) \right. \\ &\quad \left. + (p^\mu q^\nu + q^\mu p^\nu)(pq) \right] + \frac{1}{q_3^2 + M^2} [q \rightarrow p - q] , \\ N_2^{\mu\nu} &= \frac{1 - \delta_{q_3, p_3}}{(q_3 - p_3)^2(q_3^2 + M^2)} (p^2 q^\mu - qp p^\mu)(p^2 q^\nu - qp p^\nu), \end{aligned} \quad (105)$$

with their characteristic denominators. As above, the 3-dimensional integrations are performed within dimensional regularization and the resulting divergent sums are computed with heat-kernel regularization. The 3-dimensional integrations can be carried out in closed form, and the resulting expressions are given in Appendix B. The subsequent sum over the 3-momenta cannot be performed analytically due to the gluon mass.

We first discuss the regularization dependent contributions to the charged gluon self energy. The product of the two gauge terms makes the momentum sum over  $N_2^{\mu\nu}$  in Eqs.

(104), (105) convergent, while  $N_{0,1}^{\mu\nu}$  give rise to divergent momentum sums. The regulator dependent terms are

$$\Pi_{\text{gg}}^{\mu\nu}(p, p_3) = i\frac{g^2}{\pi^2} \left\{ \frac{2}{3\lambda^2} g^{\mu\nu} - \frac{11}{12} \ln \lambda \left[ (p^2 - p_3^2 + \frac{2}{11} M^2) g^{\mu\nu} - p^\mu p^\nu \right] \right\} + \dots \quad (106)$$

In addition the tadpole contribution of Fig. 4b has to be included. Evaluation of this contribution in the same scheme as above yields

$$\Pi_{\text{tp}}^{\mu\nu}(p, p_3) = i\frac{g^2}{\pi^2} \left( -\frac{2}{3\pi^2\lambda^2} + \frac{1}{6} M^2 \ln \lambda \right) g^{\mu\nu} + \dots \quad (107)$$

The quadratically divergent mass corrections appearing in the vacuum polarization and tadpole cancel each other, as does the  $M$ -dependent logarithmic divergence. The remaining divergence,

$$\Pi^{\mu\nu}(p, p_3) = \Pi_{\text{gg}}^{\mu\nu}(p, p_3) + \Pi_{\text{tp}}^{\mu\nu}(p, p_3) = i\frac{g^2}{\pi^2} \left\{ -\frac{11}{12} \ln \lambda \left[ (p^2 - p_3^2) g^{\mu\nu} - p^\mu p^\nu \right] \right\} + \dots \quad (108)$$

can be eliminated by wave function renormalization, i.e., by inclusion of a counterterm to the Lagrangian of Eq. (50)

$$\delta\mathcal{L} = -(Z_\Phi - 1) \left[ \frac{1}{2} (\partial_\mu \Phi_\nu^\dagger - \partial_\nu \Phi_\mu^\dagger) (\partial^\mu \Phi^\nu - \partial^\nu \Phi^\mu) + \partial_3 \Phi_\mu^\dagger \partial^3 \Phi^\mu \right]. \quad (109)$$

The choice

$$Z_\Phi = z_\Phi - \frac{11g^2}{12\pi^2} \ln \lambda \quad (110)$$

with finite  $z_\Phi$  ( $z_\Phi = 1$  in minimal subtraction) gives rise to a finite charged gluon propagator which (suppressing trivial color labels) can be written as

$$\tilde{D}_{\mu\nu} \approx D_{\mu\nu} + iD_{\mu\sigma} \Pi^{\sigma\rho} D_{\rho\nu} \approx \frac{z_\Phi}{p^2 - p_3^2 - z_\Phi M^2 + i\epsilon} \left[ -g_{\mu\nu} + \frac{p_\mu p_\nu}{p_3^2 + z_\Phi M^2} \right]. \quad (111)$$

Thus the divergent contributions to vacuum polarization and tadpole do not change the gauge structure of the charged gluon propagator.

The neutral gluon propagator can be discussed in the same way. The free propagator (82) does not contain a (geometrical) mass term nor is such a term generated at one loop order. Again only wave function renormalization is required.

The behaviour of the charged gluon self energy for large spacelike momenta is of interest in particular for the calculation of the Polyakov loop correlation function at small distances. As for the vacuum polarization correction to the Polyakov loop correlator calculated above, also here the leading contributions arise from the gauge terms of the gluon propagators. It is convenient to decompose the charged gluon self-energy as follows,

$$\Pi_{\text{gg}}^{\mu\nu}(p, p_3) = ig^2 \left( \left[ g^{\mu\nu} \frac{p^\mu p^\nu}{p^2} \right] \Pi_{\text{gg}}^{(1)}(p, p_3) + g^{\mu\nu} \Pi_{\text{gg}}^{(2)}(p, p_3) \right) \quad (\mu, \nu = 0, 1, 2). \quad (112)$$

This decomposition makes use of the covariance in 2+1 dimensional Minkowski space which is respected by the 2+1 dimensional residual gauge fixing as well as the regularization procedure. The leading terms in the asymptotic expansion for large spacelike momenta  $p^2 \rightarrow -\infty$  are

$$\begin{aligned}\Pi_{\text{gg}}^{(1)}(p, p_3) &\approx \frac{(-p^2)^{5/2}}{64L} \sum_{q_3 \neq p_3} \frac{1}{(q_3^2 + M^2)(q_3 - p_3)^2} , \\ \Pi_{\text{gg}}^{(2)}(p, p_3) &\approx \frac{(-p^2)^{1/2}}{32L} \left( 2 - \sum_{q_3 \neq p_3} \frac{(p_3^2 - 2q_3 p_3 - M^2)^2}{(q_3^2 + M^2)(q_3 - p_3)^2} \right) .\end{aligned}\quad (113)$$

Higher order terms are given in Appendix B. We note the difference in the leading power of  $\Pi_{\text{gg}}^{(1)}$  and  $\Pi_{\text{gg}}^{(2)}$ . The  $(-p^2)^{5/2}$  behaviour results when retaining only the gauge terms in the two gluon propagators and is therefore determined by  $N_2^{\mu\nu}$  of Eq. (105). The resulting  $p_3^{-4}$  dependence together with the  $1/L$  associated with the momentum sum requires, for dimensional reasons, the fifth power in  $p$ . Furthermore, using the transversality property of the three gluon vertex

$$V_{3,\lambda\mu\nu}(p, q, r, )p^\lambda q^\mu r^\nu = 0 , \quad (114)$$

it is easily seen that this term must be transverse, i.e., vanish after contraction with  $p_\mu$  or  $p_\nu$ . In turn, the large momentum behaviour of  $\Pi_{\text{gg}}^{(2)}$  is obtained by retaining in one of the propagators the gauge term. By simple power counting a  $p^3$  behaviour is expected. However integration over  $N_2^{\mu\nu}$  in Eq. (104) yields a vanishing coefficient.

#### 4.4 Polyakov Loop Correlator to Order $g^4$ at Large Momenta

In this section, we shall calculate the asymptotic behavior of the Polyakov loop correlator to order  $g^4$  for large momenta. As our one loop results indicate, this asymptotic behavior is determined by the gauge terms in the gluon propagators and so is the related free energy of a quark-antiquark system. On the other hand, by asymptotic freedom, a Coulomb-like quark-antiquark interaction energy is expected for sufficiently small separations. It is thus of conceptual interest how the expected  $1/r$  behavior arises given the unusual asymptotic form of the propagators.

Three of the four Feynman diagrams shown in Fig. 5 contribute to order  $g^4$  to the Polyakov loop correlator. Diagram 5d vanishes since the external vertices are linear in the independent summation variables  $k_3, q_3$  and otherwise only even powers of these variables arise. Although different from zero, diagram 5c, the tadpole insertion in the one loop diagram, is asymptotically of the same order in  $p$  as the one loop diagram and therefore subleading as will be seen. We are thus left with the self-energy 5a and vertex correction 5b. As illustrated above, the leading large momentum behavior can be analysed by distinguishing between the  $g^{\mu\nu}$  and gauge term ( $p^\mu p^\nu$ ) contributions to the gluon propagators (Eqs. (80), (82)) and classifying accordingly the contributions to a given diagram. The highest conceivable power of  $L$  of the diagrams 5a, 5b arises when retaining in all the 5 propagators the gauge terms ( $\sim (L^2)^5$ ); both double sum and external vertices contribute a factor  $L^{-2}$  giving rise to a  $L^6 p^8$  behaviour. However, the coefficient of this term vanishes due to

to the transversality of the three gluon vertex, Eq. (114). Therefore a  $g_{\mu\nu}$  contribution to at least one of the propagators has to be kept, avoiding thereby appearance of a vertex with three adjacent gauge terms. In Fig. 6 the two contributions to the diagrams 5a, 5b are shown with the marked propagator denoting the  $g_{\mu\nu}$  contribution (gauge terms otherwise). Superficially, these contributions give rise to a  $L^4 p^6$  dependence. Dimensionally regularized integration yields however a vanishing coefficient and thus at large momenta, this contribution actually behaves as  $L^2 p^4 \ln(-p^2)$ . For consistency, at this order, one also has to take into account all the terms generated from the original diagrams 5a, 5b by retaining  $g_{\mu\nu}$  in two out of the 5 propagators, dropping the  $q_3$  dependence of the denominators. This yields already a fairly large number of terms which are identified in Figs. 7 and 8. Several simplifications occur before the final evaluation: Diagram 7b vanishes in dimensional regularization, diagram 7c has a lower power of  $L$  than naive counting due to a divergent  $n$ -sum and can be discarded, and diagram 8a vanishes due to the  $k_3, q_3$  sum. Thus for the following 6 distinct subdiagrams 6a, 6b, 7a, 7d, 8b and 8c, the coefficients of the leading  $L^2 p^4 \ln(-p^2)$  terms have to be calculated. A final comment concerns the appearance of the logarithmic momentum dependence. Integration over one of the two loop momenta ( $k$ ) generates odd powers of the second loop momentum ( $(-q^2)^{n/2}$ ) which in the subsequent dimensionally regularized integration leads to poles in the  $\Gamma$  function and thereby to the standard logarithmic momentum dependence.

In a rather lengthy calculation, we have determined the individual contributions of the subdiagrams of Figs. 6 – 8. The coefficients of the (two loop) Polyakov loop correlation function which multiply the leading asymptotic term

$$\frac{ig^4 L^2}{2\pi^2} p^4 \ln(-p^2) , \quad (115)$$

are listed in Table I (diagram 7a gives zero). Adding up all the terms and including the result of the one loop calculation (Eq. (95)), we finally obtain

$$\Pi_{\text{gg}}^{33}(p)|_{1\text{-loop}} + \Pi_{\text{gg}}^{33}(p)|_{2\text{-loop}} \approx 0.32i \frac{g^2}{4\pi} L (-p^2)^{3/2} \left[ 1 - 0.043 \frac{g^2}{4\pi} L (-p^2)^{1/2} \ln(-p^2) \right]. \quad (116)$$

## 4.5 Interaction of Static Charges at Short Distances

Fourier transformation of the above result yields the short distance behavior of the Polyakov loop correlator

$$\mathcal{D}(r) \approx 0.31 \frac{ig^2 L}{\pi^2 r^6} \left( 1 + 0.67 \frac{g^2 L}{4\pi r} \right) \quad (117)$$

and thus, up to an additive constant, the free energy associated with static charges at small separations

$$V(r) \approx \frac{6}{L} \ln(\mu r) - 0.67 \frac{g^2}{4\pi} \frac{1}{r} . \quad (118)$$

We first note that the expansion parameter in this perturbative treatment of the Polyakov loop correlator is  $g^2 L/4\pi r$  and not  $g^2/4\pi$ . This is to be expected if the interaction energy contains a Coulomb-like contribution  $g^2/4\pi r$ . In this case, like in QED, expansion of the exponential  $\exp(-LV(r))$  requires

$$\frac{g^2 L}{4\pi r} \ll 1 . \quad (119)$$

For sufficiently large extensions  $L$  and by asymptotic freedom,

$$r \ll L \quad \text{and} \quad r \ll 1/\Lambda_{\text{QCD}} ,$$

we actually do expect the interaction energy to be given by

$$V(r) \sim c \frac{g^2}{4\pi r} + \frac{1}{L} v(r) + \dots \quad (120)$$

up to  $1/L$  corrections and terms of higher power in the coupling constant. It is remarkable that the expansion in the parameter (119) is generated by the gauge terms in the gluon propagators; we recognize here the intimate connection between the ultralocality property of the Polyakov loops and the presence of the gauge terms in the gluon propagators. While by ultralocality the Polyakov loop correlator gets reduced to a correlator of the composite field  $u(x_\perp)$  (cf. Eq. (48)), the higher powers of  $L/r$  in the composite field correlator can only be generated by the gauge terms. Our calculation also shows that the appearance of the combination  $\frac{g^2}{4\pi} (\frac{L}{r})^n$  with  $n = 1$  is by no means trivial. As shown above, dimensional arguments suggest  $n = 3$  or  $n = 2$  as leading terms and only due to specific properties of propagators and couplings, the corresponding coefficients turn out to be zero. In summary, the structure of our final result for the Polyakov loop correlator is in agreement with general expectations and strongly supports the consistency of the approach.

The value of the constant multiplying the Coulomb interaction further characterizes the dynamics in the  $Z_2$  symmetric phase. In the confined phase, calculation of the interaction energy either via the Polyakov loop correlator or via Wilson loop are expected to yield the same result which to lowest order and for short distances is given by the singlet potential

$$V_0(r) = -\frac{3}{4} \frac{g^2}{4\pi r} . \quad (121)$$

On the other hand, treating Polyakov loop variables as Gaussian variables and applying standard perturbation theory yields the color averaged potential ([32], [33]) with the weight given by the statistical factor,

$$V_{\text{av}}(r) = \frac{1}{4}(V_0(r) + 3V_1(r)) = O(g^4/r^2) , \quad (122)$$

i.e., to lowest order a vanishing interaction energy is obtained. Our approximative interaction energy is significantly different from this color averaged potential and rather close to the singlet potential. This is a consequence of having completely resolved the Gauss law. In a perturbative resolution, one gluon exchange is attractive in the singlet and repulsive

in the triplet channel; the interaction effects exactly cancel when taking the trace over the color spins of the static charges. With the Gauss law fully resolved, all states and operators are gauge invariant. The concept of singlet or triplet states is not meaningful anymore. The perturbative triplet states are made gauge invariant by appropriate gluon admixtures. To estimate the effect of such gluon admixtures, we change the weight in the average potential,

$$e^{-L\tilde{V}_{\text{av}}(r)} = \left( e^{3Lg^2/16\pi r} + 3e^{-L\Delta E} e^{-Lg^2/16\pi r} \right) / \left( 1 + 3e^{-L\Delta E} \right) . \quad (123)$$

$\Delta E$  is the energy necessary to produce gluons which compensate for the color of the static charges in the triplet state. If we identify this energy with the threshold of charged gluons

$$\Delta E \approx \frac{1}{L} \sqrt{\frac{4}{3}\pi^2 - 2} , \quad (124)$$

a Taylor expansion in terms of the coupling constant yields

$$\tilde{V}_{\text{av}}(r) = -0.65 \frac{g^2}{4\pi r} . \quad (125)$$

The agreement of this simple estimate with the above calculation suggests that in the  $Z_2$  symmetric phase the sector of states originating from color carrying states is shifted towards higher energies relative to the sector of states originating from perturbative singlet states. We thus arrive from this consideration of the interaction energy at short distances to conclusions very similar to those obtained in the discussion of the “perturbative” linear confinement. In both cases we find that the phase realizing the center symmetry apparently contains the seeds for non-perturbative phenomena such as the energetic suppression of colored states and a linear rise of the interaction energy with increasing separation. However, the energy scale connected with these phenomena is determined geometrically by the extension of the system rather than by non-perturbative dynamics.

## 4.6 Interaction of Static Charges in the Presence of Light Quarks

In this paragraph we shall discuss the effect of dynamical quarks on the interaction energy of static charges at large distances. Our analysis will be a perturbative one, i.e., we shall assume that the fermionic ground state is that of free fermions which satisfy the boundary conditions (23). The change from anti-periodic boundary conditions to these quasi-periodic ones accounts for the interaction with the Aharonov–Bohm fluxes generated by the ultralocal Polyakov loop variables and, as will be seen, is the crucial agent for producing the string breaking mechanism.

Starting point of our perturbative calculation is Eq. (63) which yields for the asymptotic behaviour of the interaction  $V$

$$\exp \{ -LV(r) \} \approx |\langle \Omega | u(0) | \Omega \rangle|^2 \quad (126)$$

if the order field  $u$  develops a non-vanishing vacuum expectation value. Disregarding the coupling between quarks and gluons, this vacuum expectation value has to be generated

by the quarks and according to the definition of  $u$  (Eq. (43)) is given by

$$\begin{aligned} \langle \Omega | u(x_\perp) | \Omega \rangle &= -L \langle \Omega | \bar{\psi}(x) \frac{\tau_3}{2} \gamma_3 \psi(x) | \Omega \rangle \\ &= \frac{L}{2} \left[ \langle \Omega | \bar{\chi}_\alpha(x) \gamma_3 \chi_\alpha(x) | \Omega \rangle \Big|_{\alpha=1/4} - \langle \Omega | \bar{\chi}_\alpha(x) \gamma_3 \chi_\alpha(x) | \Omega \rangle \Big|_{\alpha=-1/4} \right]. \end{aligned} \quad (127)$$

In eliminating the color dependence we have introduced fermion fields

$$\chi_\alpha(x) = \sum_{\pm s} \frac{1}{\sqrt{L}} \sum_{k_3} \int \frac{d^2 k}{2\pi} \sqrt{\frac{m}{E_k}} \left[ b(k, s) u(k, s) e^{-ikx} + d^\dagger(k, s) v(k, s) e^{ikx} \right]. \quad (128)$$

which satisfy the boundary condition

$$\chi_\alpha(x_\perp, x_3 = L) = e^{2i\pi\alpha} \chi_\alpha(x_\perp, x_3 = 0). \quad (129)$$

The divergent expression for the vacuum expectation value

$$j_3(\alpha, m, L) = \langle \Omega | \bar{\chi}_\alpha(x) \gamma_3 \chi_\alpha(x) | \Omega \rangle = \frac{1}{L} \sum_{k_3} \int \frac{d^2 k}{(2\pi)^2} \frac{2k_3}{E_k} \quad (130)$$

is evaluated by performing the integral over transverse momenta in dimensional regularization (scale  $\mu$ ,  $\omega \rightarrow 1$ )

$$j_3(\alpha, m, L) = \frac{2\mu^{2-2\omega}}{L} \frac{\Gamma\left(\frac{1}{2} - \omega\right)}{\sqrt{\pi} (4\pi)^\omega} \sum_{k_3} k_3 \left(m^2 + k_3^2\right)^{\omega - \frac{1}{2}}. \quad (131)$$

The sum over the momenta

$$k_3 = \frac{2\pi}{L} (n + \alpha) \quad (132)$$

can be carried out explicitly (cf. [34]) and yields the finite result

$$j_3(\alpha, m, L) = \frac{2m^2}{\pi^2 L} \sum_{n=1}^{\infty} \frac{\sin 2\pi n\alpha}{n} K_2(nmL). \quad (133)$$

The vacuum expectation value of the current vanishes if  $\alpha = 0$  or  $\alpha = 1/2$ , i.e., for periodic or antiperiodic boundary conditions. Only then does the spectrum of fermionic states contain parity doublets (with the exception of the parity even zero mode for  $\alpha = 0$ ). We also note that  $j_3$  changes sign with  $\alpha$ . Finally in the two limiting cases  $mL \rightarrow 0, \infty$  the following explicit expressions are obtained

$$j_3(\alpha, m, L) \approx \begin{cases} \sqrt{2} \left(\frac{m}{\pi L}\right)^{3/2} e^{-mL} \sin 2\pi\alpha & mL \gg 1 \\ \frac{4\pi}{3L^3} (\alpha - 3\alpha^2 + 2\alpha^3) & mL \ll 1 \end{cases} \quad (134)$$

Thus for asymptotic separations, the interaction energy of two static charges reaches the constant value

$$V(r) \approx 2m, \quad (135)$$

up to corrections of  $O(1/L)$ . It is remarkable that this correct form of the asymptotics of  $V$  appears at this perturbative level. In standard perturbation theory quark loops yield as in QED an Uehling type correction [35] to the Coulomb interaction  $\delta V \propto g^4 \exp(-2mr)/r$ . Perturbation theory in the center symmetric phase on the other hand yields the coupling constant independent result (135). Thus the mechanism of string breaking by pair formation is apparently present in the center symmetric phase already at the perturbative level. The calculation also displays the important role of the modification of the boundary conditions, i.e., the role of the Aharonov–Bohm fluxes. The string breaking mechanism would not be present if dynamical quarks satisfied standard anti-periodic boundary conditions, nor would it arise if the boundary conditions would not differentiate between the two color states of the quarks ( $\tau_3$  in the b.c. (23)).

## 5 Conclusions

We have presented an analysis of  $SU(2)$  Yang Mills theory and QCD with the focus on the role of the center symmetry and the dynamics of the Polyakov loops. We have carried out these investigations with a choice of the geometry where one of the spatial directions is compact. Our gauge choice consists in eliminating the corresponding spatial component of the gauge field up to the eigenvalues of the Polyakov loops winding around the compact direction. This representation of QCD at finite extension is connected by a rotation in the Euclidean with the (modified) temporal gauge representation of QCD at finite temperature. The gauge fixing procedure leading to this modified axial gauge representation has been carried out explicitly and completely. No perturbative elements are required in for eliminating redundant variables and, as a consequence, the resulting gauge fixed formulation is, in the absence of quarks, manifestly symmetric under center symmetry transformations. This is in contradistinction to perturbative elimination of redundant variables or, equivalently, perturbative treatments of gauge fixing terms and associated Faddeev–Popov determinants. Such approaches necessarily inherit the residual symmetries of the underlying  $U(1)^{N^2-1}$  rather than those of the  $SU(N)$  gauge theory and thereby generate the weak coupling phase of an Abelian theory with the dynamics of the Polyakov loops similar to those of QED. The correlation function of these variables yields, as is well known, Coulomb like interaction energies for static charges and exhibits, in next order, the phenomenon of Debye screening. On the other hand, such properties cannot be shared by a phase in which the center symmetry is realized. In such a phase, the Polyakov loop expectation value necessarily vanishes, signaling an infinite free energy of a single static quark. Concomitantly the center symmetric phase does not screen color charges; perturbative evaluation of the Polyakov loop correlator yields imaginary masses for these degrees of freedom indicating instability of the perturbative Polyakov loop vacuum. The physical vacuum has been shown to be the vacuum of ultralocal rather than Gaussian degrees of freedom, i.e., degrees of freedom which are essentially inert and can propagate only via their coupling to other degrees of freedom.

This property of ultralocality of the Polyakov loop variables induces significant changes in the formalism. Most importantly, it effectively identifies propagator and self-energy,

i.e., the connected with the one particle irreducible 2-point function. With this structural change, confining interactions emerge as naturally from the propagator as do Yukawa or Coulomb potentials in the case of Gaussian variables. This mechanism is reminiscent of the emergence of confinement by formation of Gribov horizons [1]. In both cases it is the limitation in phase space, i.e., the finite range of the functional integration, which is the source of confinement phenomena. Essential differences arise by the gauge choice. In the (modified) axial gauge, Gribov horizons appear for elementary degrees of freedom while in Coulomb or Lorentz gauge, they restrict the phase space of composite variables [36, 37, 38]. Furthermore, with the identification of propagators and self energies, simple relations could be established between properties of the confining interaction between static quarks and the spectrum of gluonic states. In particular a non-vanishing value of the string constant in the thermodynamic limit has been shown to require the presence of an energy gap in the sector of gluonic excitations which are coupled to Polyakov loops. In the limit of infinite extension this gap must diverge. Thereby this sector of the Hilbert space gets effectively decoupled from low lying excitations. A similar analysis has been carried through for the Polyakov loop in the adjoint representation. The center symmetry does not force the vacuum expectation value of the adjoint Polyakov loop to vanish and thus, depending on the dynamics, a Coulomb or Yukawa potential acting between adjoint color charges results. The behaviour under center symmetry transformations constitutes the crucial difference between the states which contribute to the correlation function of the Polyakov loops in either the fundamental or the adjoint representation.

These results suggest the following interpretation of the phases of the Yang–Mills theory. For sufficiently large extension, the Hilbert space of physical states factorizes into the sector of “low-lying” states which are even under center symmetry transformations, and the sector of odd states which is separated from the center symmetric ground state by an energy gap  $\Delta E_- = \sigma L$  determined by extension and string constant and diverging in the thermodynamic limit. These two sectors are completely disconnected. Furthermore, as follows from the absence of long range strong interactions and as confirmed by lattice calculations, a gap must be present also in the sector of even states; it is given by the lowest glueball mass  $\Delta E_+ = M_g$ . With decreasing extension (or equivalently increasing temperature) the gap in the sector of odd states decreases till it reaches a value  $\Delta E_- \approx \sigma T_c \approx 1\text{GeV} \approx \Delta E_+$ . At this extension it apparently becomes energetically favourable for the system to break the center symmetry, allowing thereby for mixing of even and odd states. This in turn implies the vanishing of the string tension. Due to the change in symmetry, this transition has to occur in a discontinuous way.

Not only is the property of ultralocality of fundamental importance for the structure of the center symmetric phase, it also is an essential ingredient for establishing perturbation theory in the center symmetric phase. After integrating out the Polyakov loops, expansion in the coupling constant is possible without ruining the center symmetry. As a consequence, certain confinement like properties can be obtained already within perturbation theory. In particular a linear rise in the interaction energy of static color charges is present perturbatively. Quantitatively, the spectrum of gluonic excitations is poorly described in perturbation theory and does not yield a realistic value of the string constant. Perturbation theory is however sufficient to reproduce the correct asymptotics of

the interaction energy if dynamical quarks are present. Unlike ordinary perturbation theory which yields a  $1/r$  behavior modified by a Uehling type potential arising from quark loops, perturbation theory in the center symmetric phase predicts correctly the interaction energy of asymptotically separated static color charges to be given by twice the quark mass. In addition to these confinement like properties originating from the Polyakov loop dynamics, the perturbative center symmetric phase displays non-trivial properties of other gluonic degrees of freedom. In the process of elimination of the Polyakov loops, charged gluons, i.e., gluons which are associated with the non-diagonal generators of the  $SU(N)$  symmetry, acquire a mass term and become coupled to space-time independent Aharonov–Bohm fluxes. These modifications of the gluon dynamics are independent of the coupling constant and geometrical, i.e., dependent on the extension. The Aharonov–Bohm fluxes suppress Debye screening in the center-symmetric phase. Presence of a mass term for charged gluons and its absence for neutral gluons can be seen as a first hint for Abelian dominance of long range phenomena. It is remarkable that realization of the center symmetry by proper gauge fixing yields these characteristics of the confined phase.

With the center symmetry realized, novel conceptual problems also arise in the application of perturbation theory to short distance phenomena if confined variables are involved. This has been illustrated in our discussion of the interaction energy of static charges if calculated via the Polyakov loop correlator. Clearly, irrespective of the realization of the center symmetry, whenever the separation of the charges  $r$  is small, i.e.,  $r \ll L = 1/T$  and  $1/r \gg \Lambda_{\text{QCD}}$ , this interaction energy must be given by lowest order perturbation theory. However, perturbative evaluation of the Polyakov loop correlator does not reproduce the expected Coulomb-like behaviour, but rather seems to suggest a  $1/r^2$  dependence at short distances. However perturbation theory not only involves the small coupling constant  $g^2/4\pi \ll 1$  but also the quantity  $g^2 L/4\pi r = g^2/4\pi T r$  which becomes large at short distances and thereby turns the calculation of the Polyakov loop correlator into a strong coupling problem. The Polyakov loop self-energies are dominated at large momenta not by the familiar  $p^2$  term with its standard logarithmic corrections but rather by extension or temperature dependent  $(g^2 p L)^n p^2$  corrections. These unusual contributions to the self-energy originate from the “gauge terms” of the gluon propagators. Their presence is necessary for generating the proper short distance behavior, as is the ultralocality of the Polyakov loops.

Our investigations represent a first, exploratory analysis of the center symmetric phase of QCD. The focus has been on the consequences of the realization of the center symmetry and in particular on those properties which are reminiscent of the confining phase of QCD and which emerge already at the perturbative level. Nevertheless the wealth of non-perturbative phenomena cannot be accounted for at this perturbative level. Only Polyakov loop variables exhibit phenomena associated with confinement. Although other degrees of freedom are significantly affected by the realization of the center symmetry, confinement of these degrees of freedom is not manifest, nor does it seem to be within the reach of perturbation theory. Self couplings of the gluonic degrees of freedom may generate these non-perturbative dynamics. We have however not been able to identify specific mechanisms. Alternatively, it might be necessary to extend the formalism by inclusion of singular gauge field configurations when integrating out the Polyakov loop

variables. Our implicit restriction to smooth gauge fields may not be justified. When diagonalizing the Polyakov loops, ambiguities arise whenever the Polyakov loop passes through the center of the group. These ambiguities yield the monopole like singularities characteristic for Abelian projected QCD. Condensation of these monopoles could then lead, via the dual Meissner effect, to confinement of gluonic degrees of freedom also where center symmetry does not dictate it. We are in the process of studying the necessary modifications of the formalism.

Extension of our investigation to  $SU(3)$  or more generally  $SU(N)$  Yang Mills theory is of interest. As indicated in our work, the formalism can easily be extended to higher groups. The construction of the effective Lagrangian in its Abelian projected form is straightforward but technically more involved (most of the necessary modifications have been worked out for  $SU(3)$  color in [27]). The structure of the center symmetric phase is, in general, more complex than for  $SU(2)$  color. In particular, the  $Z_3$  center symmetry of  $SU(3)$  Yang Mills theory allows for a confinement-deconfinement transition which is first order and may lead to formation of domains. Existence of such domains, the  $Z_N$  bubbles, is a controversial issue (cf. [39], [40]) and our formalism may provide new perspectives. Unlike at finite temperature, the center symmetry is an ordinary symmetry at finite extension. It is canonically described by an operator which commutes with the Hamiltonian and thus formation of  $Z_N$  bubbles under compression of the system is conceptually simpler than bubble formation when heating the system. Furthermore, application of our techniques to the large  $N$ -limit might provide the possibility to study the weak coupling, confining phase which e.g. has been invoked to connect large  $N$ -QCD with string theory [41].

Our final remarks concern the description of the deconfined phase. With the center symmetry realized, the transition to the deconfined phase becomes, as it should be, a dynamical issue. From this point of view, the standard procedure to reach the deconfined phase by perturbative gauge fixing or equivalently by perturbative resolution of the Gauss law appears to be rather arbitrary. Perturbative gauge fixing prevents the system from reaching the confined phase at the expense of not only breaking the center symmetry but also violating other constraints imposed by local gauge invariance. Problems associated with such a procedure appear explicitly in the standard derivation of Debye screening in temporal or modified temporal gauge. Naive treatment of the Polyakov loop variables as Gaussian variables is not legitimate at any temperature. Also in the deconfined phase, these degrees of freedom have, as angular variables, a finite range of definition and remain ultralocal. On physical grounds, however, we expect Debye screening to be a reasonable approximate concept at sufficiently high temperatures. As in the Debye–Hückel theory where, in conflict with the Gauss law, one shows screening of a test charge when introduced into a neutral system, in QCD one apparently might have to allow similarly for certain violations of the Gauss law rather than to insist on its exact implementation. However the non-linearities of the Gauss law may invalidate such an approximation in QCD (inert background charges which compensate for violations of the Gauss law do not exist) and lead to inconsistencies in higher order. The divergence of finite temperature QCD perturbation theory beyond  $g^6$  [31] indicates the failure of such an approach and, in agreement with results from lattice QCD (cf. [42]), suggests the deconfined phase and its screening properties not to be accessible by standard perturbation theory ([43], [44]).

Although perturbative investigations are not sufficient to describe the dynamics of the confinement-deconfinement phase transition, they nevertheless are useful in identifying properties which necessarily change when the center symmetry gets spontaneously broken. These can be used in conjunction with stability requirements to characterize the high temperature deconfined phase [45].

We thank V.L. Eletskii and A.C. Kalloniatis for valuable discussions. This work has been supported by the Bundesministerium für Bildung, Wissenschaft, Forschung und Technologie.

# Appendix A: Electron Self-Energy in Axial Gauge

In this appendix we show in lowest order perturbation theory that the electron self energy in axial gauge is dominated at large (transverse) momenta by the gauge terms in the propagator. The photon propagator in axial gauge QED coincides for  $p_3 \neq 0$  with the neutral gluon propagator of SU(2)-QCD (cf. Eq. (82))

$$D_{\mu\nu}(p, p_3) = \frac{1}{p^2 - p_3^2 + i\epsilon} \left[ -g_{\mu\nu} + p_\mu p_\nu (1 - \delta_{p_3,0}) \frac{1}{p_3^2} + p_\mu p_\nu \delta_{p_3,0} (1 - \xi) \frac{1}{p^2 + i\epsilon} \right] \quad (\text{A.1})$$

with

$$p_3 = \frac{2\pi n}{L}, \quad (\text{A.2})$$

but unlike QCD contains a 33-component describing photons polarized in the 3 direction and propagating in transverse space,

$$D_{33}(p) = \frac{\delta_{p_3,0}}{p^2 + i\epsilon}. \quad (\text{A.3})$$

We consider the contribution to the self-energy which is generated by the second term in the propagator (A.1),

$$i\delta\Sigma(p) = e^2 \frac{1}{L} \sum_{q_3} \int \frac{d^3q}{(2\pi)^3} \frac{(1 - \delta_{q_3,0})}{q^2 - q_3^2 + i\epsilon} \frac{q_\mu q_\nu}{q_3^2} \frac{\gamma^\mu [(\not{p} - \not{q}) + m] \gamma^\nu}{(p - q)^2 - (p_3 - q_3)^2 - m^2 + i\epsilon}. \quad (\text{A.4})$$

Using the techniques developed in the main section, the leading term for large transverse momenta can straightforwardly be determined with the result

$$\delta\Sigma(p) \approx \frac{e^2}{192} \not{p}_\perp L \sqrt{-p_\perp^2}. \quad (\text{A.5})$$

Thus in axial gauge at large transverse momenta, the first order correction exceeds the free self-energy by a power of  $p_\perp L$ .

Such an unusual large  $p$  asymptotics which, in the electron self energy, is generated by the gauge terms of the photon propagator, is absent if we start (before gauge fixing) from a gauge invariant quantity such as the electron two point function with an appropriate gauge string insertion,

$$\tilde{S}(x, y)_{\alpha\beta} = i \langle 0 | T(\bar{\psi}_\beta(y) \exp \left\{ -i e \int_x^y ds^\mu A_\mu \right\} \psi_\alpha(x)) | 0 \rangle. \quad (\text{A.6})$$

To order  $e^2$ , this two point function is given by

$$\begin{aligned} \tilde{S}(x, y) &= S_F(x, y) \left( 1 - i \frac{e^2}{2} \int_0^1 \frac{dx^\mu}{ds} \int_0^1 \frac{dx^\nu}{ds'} D_{\mu\nu}(x(s), x(s')) \right) \\ &+ e^2 \int_0^1 \frac{dx^\mu}{ds} \int d^4z D_{\mu\lambda}(x(s), z) S_F(x, z) \gamma^\lambda S_F(z, y) \\ &+ i \frac{e^2}{2} \int d^4z d^4z' D_{\mu\lambda}(z, z') [S_F(x, z') \gamma^\nu S_F(z', z) \gamma^\mu S_F(z, y) \\ &+ S_F(x, z) \gamma^\mu S_F(z, z') \gamma^\nu S_F(z', y)] \end{aligned} \quad (\text{A.7})$$

with  $x^\mu(s)$  parametrizing the gauge string. We split the photon propagator

$$D_{\mu\nu}(q) = D_{\mu\nu}^{\text{F}}(q) + D_{\mu\nu}^{\text{ax}}(q) \quad \mu, \nu = 0..3 \quad (\text{A.8})$$

into the Feynman gauge propagator

$$D_{\mu\nu}^{\text{F}}(q) = \frac{-g_{\mu\nu}}{q^2 + i\epsilon} \quad (\text{A.9})$$

and the contributions from the axial gauge terms,

$$D_{\mu\nu}^{\text{ax}}(q) = q_\mu d_\nu + q_\nu d_\mu, \quad (\text{A.10})$$

with

$$d_\mu(q) = (1 - \delta_{q_3,0}) \frac{1}{2q^2 q_3^2} q_\mu (1 - \delta_{\mu,3}) + \delta_{q_3,0} \frac{q_\mu}{(q^2 + i\epsilon)^2} (1 - \xi). \quad (\text{A.11})$$

To this order in perturbation theory,  $\tilde{S}$  (Eq. (A.7)) depends linearly on the photon propagator and therefore can be decomposed into contributions from the Feynman gauge photon propagator and axial gauge terms, respectively,

$$\tilde{S}(x, y) = S_{\text{F}}(x, z) + \tilde{S}^{\text{F}}(x, y) + \tilde{S}^{\text{ax}}(x, y). \quad (\text{A.12})$$

Denoting by  $\tilde{s}^i$  the contributions to  $\tilde{S}^{\text{ax}}(x, y)$  with  $i$  ( $=0,1,2$ ) gauge strings,

$$\tilde{S}^{\text{ax}}(x, y) = \sum_{i=0,1,2} \tilde{s}^i(x, y), \quad (\text{A.13})$$

we find

$$\tilde{s}^0(x, y) = ie^2 \int d^4z S_{\text{F}}(x, z) \gamma^\mu S_{\text{F}}(z, y) [d_\mu(x - z) + d_\mu(z - y)] \quad (\text{A.14})$$

$$\begin{aligned} \tilde{s}^1(x, y) &= ie^2 \int (d_\nu(y - z) - d_\nu(x - z)) d^4z S_{\text{F}}(x, z) \gamma^\nu S_{\text{F}}(x, y) \\ &\quad - e^2 \int_0^1 \frac{dx^\mu}{ds} ds (d_\mu(x(s) - y) - d_\mu(x(s) - x)) S_{\text{F}}(x, y) \end{aligned} \quad (\text{A.15})$$

$$\tilde{s}^2(x, y) = -ie^2 \int_0^1 \frac{dx^\nu}{ds} (d_\nu(y - x(s)) + d_\nu(x(s) - x)) \quad (\text{A.16})$$

and thus

$$\tilde{S}^{\text{ax}}(x, y) = 0. \quad (\text{A.17})$$

In the above equations,  $d_\mu(x)$  denotes the Fourier transformed gauge terms (A.11). In the derivation, we have applied the equation of motion of  $S_{\text{F}}$  and thereby made use of the continuity equation. Our result implies the independence of the large  $p$  asymptotics of  $\tilde{S}(x, y)$  of the extension  $L$ , provided of course  $L$  is not reintroduced by the choice of the gauge string (e.g. if  $x^\mu(s)$  is a path winding around the compact direction).

## Appendix B: One Loop Gluon Self Energy for SU(2)

Of interest for us are the self energies of neutral, “electric” ( $a_3$ ) and charged, “magnetic” ( $A_{0,1,2}$ ) gluons, which will be given in all detail. The results for neutral, “magnetic” gluons can be inferred from the charged ones as indicated below.

### B.1 Gluon Loop, Exact Results

Definition:

$$\begin{aligned}\Pi_{\text{gg}}^{\mu\nu}(p, p_3) &= \frac{ig^2}{4\pi L} \left( \left[ g^{\mu\nu} - \frac{p^\mu p^\nu}{p^2} \right] \Pi_{\text{gg}}^{(1)}(p, p_3) + g^{\mu\nu} \Pi_{\text{gg}}^{(2)}(p, p_3) \right) \quad (\mu, \nu = 0, 1, 2) \\ \Pi_{\text{gg}}^{33}(p) &= \frac{ig^2}{4\pi L} g^{33} \Pi_{\text{gg}}^{(3)}(p)\end{aligned}\tag{B.1}$$

Parametrization:

$$\begin{aligned}\Pi_{\text{gg}}^{(i)} &= \sum' \left\{ A_i \ln \left( \frac{x+y+P}{x+y-P} \right) + B_i \right\} e^{-\lambda x_0} + C_i \quad (i = 1, 2) \\ \Pi_{\text{gg}}^{(3)} &= \sum \left\{ A_3 \ln \left( \frac{2x+P}{2x-P} \right) + B_3 \right\} e^{-\lambda x_0}\end{aligned}\tag{B.2}$$

We use the following notation:

$$\begin{aligned}P &= \sqrt{p^2} \\ x &= \sqrt{q_3^2 + M^2} \\ x_0 &= |q_3| \\ y &= |q_3 - p_3| \\ z &= \sqrt{p_3^2 + M^2} \\ q_3 &= \frac{2\pi}{L} \left( n + \frac{1}{2} \right)\end{aligned}\tag{B.3}$$

The summation with a prime runs over all  $n$  such that  $q_3 \neq p_3$ . A heat kernel regularization is used. The sums cannot be performed analytically in general. The value for the charged gluon mass is

$$M^2 = \left( \frac{\pi^2}{3} - 2 \right) \frac{1}{L^2}\tag{B.4}$$

Results for the coefficients  $A_i, B_i, C_i$ :

$$\begin{aligned}A_1 &= -\frac{1}{16} \left\{ \frac{P^5}{x^2 y^2} + 4P^3 \left( \frac{1}{x^2} + \frac{1}{y^2} \right) - 8P \left( \frac{x^2}{y^2} + \frac{y^2}{x^2} + 3 \right) \right. \\ &\quad \left. - \frac{16}{P} (x^2 + y^2) + \frac{3}{P^3} \left( \frac{x^6}{y^2} + \frac{y^6}{x^2} + 4x^4 + 4y^4 - 10x^2 y^2 \right) \right\}\end{aligned}\tag{B.5}$$

$$B_1 = \frac{(x+y)}{8} \left\{ \frac{P^4}{x^2 y^2} - P^2 \left( \frac{1}{x^2} + \frac{1}{y^2} - \frac{6}{xy} \right) + \left( \frac{x^2}{y^2} + \frac{y^2}{x^2} - \frac{4x}{y} - \frac{4y}{x} - 2 \right) + \frac{3}{P^2} \left( \frac{x^4}{y^2} + \frac{y^4}{x^2} - \frac{2x^3}{y} - \frac{2y^3}{x} + 7x^2 + 7y^2 - 12xy \right) \right\} \quad (\text{B.6})$$

$$C_1 = -\frac{1}{8} \left( \frac{3P^3}{z^2} - 13P - \frac{7z^2}{P} + \frac{9z^4}{P^3} \right) \ln \left( \frac{z+P}{z-P} \right) + \frac{1}{4} \left( \frac{3P^2}{z} - 4z + \frac{9z^3}{P^2} \right) \quad (\text{B.7})$$

$$A_2 = \frac{(y^2 - x^2)^2}{8} \left\{ \frac{P}{x^2 y^2} - \frac{2}{P} \left( \frac{1}{x^2} + \frac{1}{y^2} \right) + \frac{1}{P^3} \left( \frac{x^2}{y^2} + \frac{y^2}{x^2} + 6 \right) \right\} \quad (\text{B.8})$$

$$B_2 = -\frac{(x+y)}{12} \left\{ \frac{3x^2}{y^2} + \frac{3y^2}{x^2} - 22 + \frac{3}{P^2} \left( \frac{x^4}{y^2} + \frac{y^4}{x^2} \frac{2x^3}{y} - \frac{2y^3}{x} + 7x^2 + 7y^2 - 12xy \right) \right\} \quad (\text{B.9})$$

$$C_2 = -\frac{1}{4} \left( P - \frac{2z^2}{P} - \frac{3z^4}{P^3} \right) \ln \left( \frac{z+P}{z-P} \right) + \frac{1}{6} \left( 11z - \frac{9z^3}{P^2} \right) \quad (\text{B.10})$$

$$A_3 = -\frac{x_0^2}{2} \left( \frac{P^3}{x^4} - \frac{4P}{x^2} + \frac{8}{P} \right) \quad (\text{B.11})$$

$$B_3 = 2x_0^2 \frac{P^2}{x^3} \quad (\text{B.12})$$

For neutral, magnetic gluons,  $\Pi_{\text{gg}}^{\mu\nu}$  can be taken over with the following modifications: No summation restriction in Eq. (B.2), interpret  $y$  as

$$y = \sqrt{(q_3 - p_3)^2 + M^2}, \quad (\text{B.13})$$

and put all  $C_i = 0$ .

## B.2 Tadpole

Definition:

$$\Pi_{\text{tp}}^{\mu\nu}(p, p_3) = \frac{ig^2}{4\pi L} g^{\mu\nu} \Pi_{\text{tp}}^{(\perp)} \quad (\mu, \nu = 0, 1, 2) \quad (\text{B.14})$$

$$\Pi_{\text{tp}}^{33}(p) = \frac{ig^2}{4\pi L} g^{33} \Pi_{\text{tp}}^{(3)}$$

Parametrization:

$$\Pi_{\text{tp}}^{(\perp)} = -\frac{4}{3} \sum (x+y) e^{-\lambda x_0} \quad (\text{B.15})$$

$$\Pi_{\text{tp}}^{(3)} = -4 \sum x e^{-\lambda x_0} \quad (\text{B.16})$$

Result (B.15) is valid for neutral magnetic gluons, provided we interpret  $y$  according to (B.13).

### B.3 Isolating Divergencies in the Sums

To get convergent sums, add and subtract the following sums derived from the large  $x$  behaviour of the above results:

$$\begin{aligned}
\Delta\Pi_{\text{gg}}^{(1)} &= \frac{11}{3}P^2 \sum \frac{1}{x_0} \\
\Delta\Pi_{\text{gg}}^{(2)} &= \left(-\frac{11}{3}p_3^2 + \frac{2}{3}M^2\right) \sum \frac{1}{x_0} + \frac{8}{3} \sum x_0 \\
\Delta\Pi_{\text{gg}}^{(3)} &= \left(\frac{11}{3}P^2 + 2M^2\right) \sum \frac{1}{x_0} - 4 \sum x_0 \\
\Delta\Pi_{\text{tp}}^{(\perp)} &= -\frac{2}{3}M^2 \sum \frac{1}{x_0} - \frac{8}{3} \sum x_0 \\
\Delta\Pi_{\text{tp}}^{(3)} &= -2M^2 \sum \frac{1}{x_0} - 4 \sum x_0
\end{aligned} \tag{B.17}$$

Notice that

$$\Delta\Pi_{\text{gg}}^{(2)} + \Delta\Pi_{\text{tp}}^{(\perp)} = -\frac{11}{3}p_3^2 \sum \frac{1}{x_0}, \tag{B.18}$$

i.e., the quadratic divergence and the  $M$ -dependence of the logarithmic divergence are cancelled. In  $\Pi^{(3)}$ , the quadratic divergence persists,

$$\Delta\Pi_{\text{gg}}^{(3)} + \Delta\Pi_{\text{tp}}^{(3)} = \frac{11}{3}P^2 \sum \frac{1}{x_0} - 8 \sum x_0. \tag{B.19}$$

However, this does not enter in our framework anyway. The relevant heat-kernel regularized sums are

$$\begin{aligned}
\sum \frac{1}{x_0} e^{-\lambda x_0} &= \frac{L}{\pi} \ln\left(\frac{2L}{\pi\lambda}\right) \\
\sum x_0 e^{-\lambda x_0} &= \frac{L}{\pi\lambda^2} + \frac{\pi}{6L}
\end{aligned} \tag{B.20}$$

For neutral magnetic gluons, the results are the same as for charged ones.

### B.4 Asymptotics for Large, Spacelike Momenta

We consider the full self energy (gluon loop and tadpole) with the following definitions, cf. Eqs. (B.1), (B.15),

$$\begin{aligned}
\Pi^{\mu\nu} &= \Pi_{\text{gg}}^{\mu\nu} + \Pi_{\text{tp}}^{\mu\nu} \\
\Pi^{(1)} &= \Pi_{\text{gg}}^{(1)} \\
\Pi^{(2)} &= \Pi_{\text{gg}}^{(2)} + \Pi_{\text{tp}}^{(\perp)} \\
\Pi^{(3)} &= \Pi_{\text{gg}}^{(3)} + \Pi_{\text{tp}}^{(3)}
\end{aligned} \tag{B.21}$$

For spacelike momenta, we introduce

$$P = i\bar{P}. \tag{B.22}$$

The gluon mass prevents us from deriving closed analytical results. Therefore we split the calculation up as follows:

$$\Pi^{(i)}[M] = \Pi^{(i)}[0] + \left( \Pi^{(i)}[M] - \Pi^{(i)}[0] \right) \quad (\text{B.23})$$

For the  $M = 0$  part, we get the following results where terms of order less than  $\bar{P}$  are only retained if they involve the cut-off parameter,

$$\begin{aligned} \Pi^{(1)}[0] &\approx \frac{\pi \bar{P}^5}{48 p_3^4} \left( (p_3 L_3)^2 - 9 \right) - \frac{\pi \bar{P}^3}{24 p_3^2} \left( 3 + 2 (p_3 L_3)^2 \right) \\ &\quad + \frac{L_3 \bar{P}^2}{9\pi} \left\{ -4 + 2\pi p_3 L_3 + 33 \left( \ln \frac{\lambda \bar{P}}{2} + \gamma \right) + 12 \ln \frac{\bar{P} L_3}{2\pi} \right. \\ &\quad \left. - 12 \left[ \psi \left( \frac{p_3 L_3}{\pi} \right) + \frac{p_3 L_3}{\pi} \psi' \left( \frac{p_3 L_3}{\pi} \right) \right] \right\} + \frac{\pi \bar{P}}{24} \left( 9 - 4 (p_3 L_3)^2 \right) + \text{O}(\ln \bar{P}) \end{aligned} \quad (\text{B.24})$$

$$\begin{aligned} \Pi^{(2)}[0] &\approx \frac{\pi \bar{P}}{24} \left( 3 - (p_3 L_3)^2 \right) + \frac{11 L_3 p_3^2}{3\pi} \ln \lambda + \text{O}(\ln \bar{P}) \\ \Pi^{(3)}[0] &\approx -\frac{\pi L_3^2 \bar{P}^3}{8} + \frac{L_3 \bar{P}^2}{9\pi} \left\{ 33 \left( \ln \frac{\lambda \bar{P}}{2} + \gamma \right) + 1 \right\} - \frac{8 L_3}{\pi \lambda^2} + \text{O}(1) \end{aligned} \quad (\text{B.25})$$

The differences

$$\Pi^{(i)}[M] - \Pi^{(i)}[0] = \sum_n \mathcal{S}_n^{(i)} \bar{P}^n \quad (\text{B.26})$$

have to be evaluated numerically. The  $\mathcal{S}_n^{(i)}$  are given by

$$\begin{aligned} \mathcal{S}_1^{(1)} &= -\frac{\pi}{2} \sum' \left\{ \frac{1}{y^2} (x^2 - x_0^2) + y^2 \left( \frac{1}{x^2} - \frac{1}{x_0^2} \right) \right\} \\ \mathcal{S}_2^{(1)} &= \frac{2}{3} \sum' \left\{ \frac{1}{y^2} (x - x_0) + y \left( \frac{1}{x^2} - \frac{1}{x_0^2} \right) \right\} \\ \mathcal{S}_3^{(1)} &= -\frac{3\pi}{8} \left( \frac{1}{z^2} - \frac{1}{z_0^2} \right) - \frac{\pi}{4} \sum' \left( \frac{1}{x^2} - \frac{1}{x_0^2} \right) \\ \mathcal{S}_5^{(1)} &= \frac{\pi}{16} \sum' \frac{1}{y^2} \left( \frac{1}{x^2} - \frac{1}{x_0^2} \right) \\ \mathcal{S}_1^{(2)} &= \frac{1}{4} \mathcal{S}_1^{(1)} \\ \mathcal{S}_1^{(3)} &= -2\pi \sum x_0^2 \left( \frac{1}{x^2} - \frac{1}{x_0^2} \right) \\ \mathcal{S}_3^{(3)} &= -\frac{\pi}{2} \sum x_0^2 \left( \frac{1}{x^4} - \frac{1}{x_0^4} \right) \end{aligned} \quad (\text{B.27})$$

All  $\mathcal{S}_n^{(i)}$  for  $n \geq 1$  not listed here are zero.

## References

- [1] V.N. Gribov, *Nucl. Phys. B* **139** (1978), 1.
- [2] G. 't Hooft, *Nucl. Phys. B* **190** (1981), 455.
- [3] L. Susskind, *Phys. Rev. D* **20** (1979), 2610.
- [4] L. McLerran and B. Svetitsky, *Phys. Lett. B* **98** (1981), 195.
- [5] J. Kuti, J. Polonyi, and K. Szlachanyi, *Phys. Lett. B* **98** (1981), 199.
- [6] A. Polyakov, *Lectures given at International Center for Theoretical Physics*, ICTP report IC/78/4 (1978), unpublished.
- [7] G. 't Hooft, *Nucl. Phys. B* **153** (1979), 141.
- [8] B. Svetitsky, *Phys. Rep.* **132** (1986), 1.
- [9] L.D. Faddeev and V.N. Popov, *Phys. Lett. B* **25** (1967), 29.
- [10] J. Schwinger, *Phys. Rev.* **130** (1963), 402.
- [11] A. Ukawa, *Nuclear Physics B (Proc. Suppl.)* **53** (1997), 106.
- [12] T. Applequist and J. Carazzone, *Phys. Rev. D* **11** (1975), 2856.
- [13] T. Applequist and R.D. Pisarski, *Phys. Rev. D* **23** (1981), 2305.
- [14] D.J. Gross, R.D. Pisarski, and L.G. Yaffe, *Rev. Mod. Phys.* **53** (1981), 43.
- [15] D.J. Toms, *Phys. Rev. D* **21** (1980), 928.
- [16] V. Koch, E.V. Shuryak, G.E. Brown, and A.D. Jackson, *Phys. Rev. D* **46** (1992), 3169.
- [17] A.P. Young, *Nucl. Phys. B (Proc. Suppl.)* **42** (1995), 201.
- [18] S.L. Sondhi, S.M. Girvin, J.P. Carini, and D. Shahar, *Rev. Mod. Phys.* **69** (1997), 315.
- [19] T. Reisz, *Z. Phys. C* **53** (1992), 169.
- [20] F. Lenz, H.W.L. Naus, and M. Thies, *Ann. Phys.* **233** (1994), 317.
- [21] F. Lenz, E.J. Moniz, and M. Thies, *Ann. Phys.* **242** (1995), 429.
- [22] H. Reinhardt, *Phys. Rev. D* **55** (1997), 2331.
- [23] N. Weiss, *Phys. Rev. D* **24** (1981), 475.
- [24] K. Kajantie and J. Kapusta, *Nucl. Phys. B* **160** (1985), 477.

- [25] K.A. James and P.V. Landshoff, *Phys.Lett. B* **251** (1990), 167.
- [26] G. Leibbrandt and M. Staley, *Nucl. Phys. B* **428** (1994), 469.
- [27] F. Lenz, M. Shifman, and M. Thies, *Phys. Rev. D* **51** (1995), 7060.
- [28] K. Amemiya and H. Suganuma, [hep-lat/9712028](#).
- [29] J. Engels, F. Karsch, and K. Redlich, *Nucl. Phys. B* **435** (1995), 295.
- [30] P.V. Landshoff, *Phys. Lett. B* **169** (1986), 69.
- [31] A.D. Linde, *Phys. Lett. B* **96** (1980), 289.
- [32] S. Nadkarni, *Phys. Rev. D* **33** (1986), 3738.
- [33] S. Nadkarni, *Phys.Rev.D* **34** (1986), 3904.
- [34] E. Elizalde *et al.*, “Zeta Regularization Techniques with Applications”, World Scientific, Singapore, 1994.
- [35] E.A. Uehling, *Phys. Rev.* **48** (1935), 55.
- [36] M. Lüscher, *Nucl. Phys.* **B219** (1983), 233.
- [37] D. Zwanziger, [hep-th/9710157](#).
- [38] P. van Baal, [hep-th/9711070](#).
- [39] A.V. Smilga, *Ann. Phys.* **234** (1994), 1.
- [40] T. Bhattacharya, A. Gocksch, and C. Korthals Altes, *Nucl. Phys. B* **383** (1992), 497.
- [41] J. Polchinski, *Phys. Rev. Lett.* **68** (1992), 1267.
- [42] G. Boyd, J. Engels, F. Karsch, E. Laermann, C. Legeland, M. Lütgemeier and B. Petersson, *Nucl. Phys. B* **469** (1996), 419.
- [43] E. Braaten and A. Nieto, *Phys. Rev. D* **51** (1995), 6990.
- [44] E. Braaten, *Phys. Rev. Lett.* **74** (1995), 2165.
- [45] V.L. Eletsky, A.C. Kalloniatis, F. Lenz and M. Thies, [hep-ph/9711230](#)

**Table I: Contributions of 2-loop subdiagrams**

diagram	value
6a	-0.67555E-03
6b	-0.10516E-02
7d	-0.15106E-03
8b	0.14243E-03
8c	0.12037E-04

# Figure Captions

- Fig. 1** One loop diagrams contributing to  $\Pi_{33}$ : Tadpole (a), ghost loop (b), gluon loop (c). Notice the different line shapes for Polyakov loop variables and charged gluons used throughout.
- Fig. 2** A typical higher order diagram involving ghosts and Polyakov loop variables.
- Fig. 3** One loop contribution to Polyakov loop correlator. The gluon-Polyakov loop vertices are the shaded blobs.
- Fig. 4** Gluon two point function to one loop. This and the following diagrams pertain to the effective theory after integrating out the Polyakov loops. Gluon loop (a) and tadpole (b).
- Fig. 5** Two loop Feynman diagrams contributing to Polyakov loop correlator.
- Fig. 6** Contributions obtained from diagrams 5a, 5b by keeping the gauge terms in the propagators everywhere except where the gluon line is marked. Here,  $g_{\mu\nu}$  term appears in one propagator only.
- Fig. 7** Like Fig. 6a, but keeping the  $g_{\mu\nu}$  term in two gluon propagators in all possible ways in the two loop self energy diagram.
- Fig. 8** Like Fig. 7, but for the two loop vertex correction diagram.

Figure 1

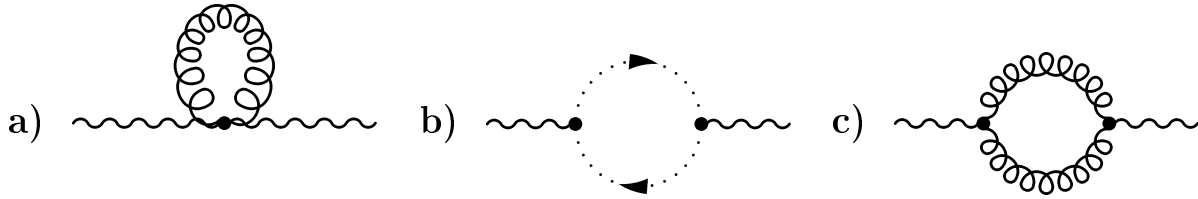


Figure 2

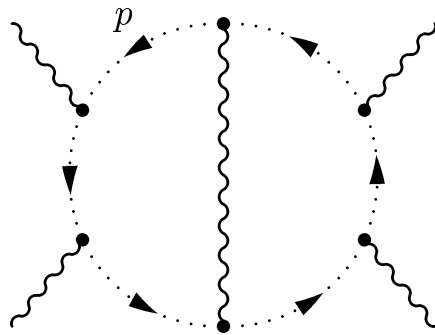


Figure 3

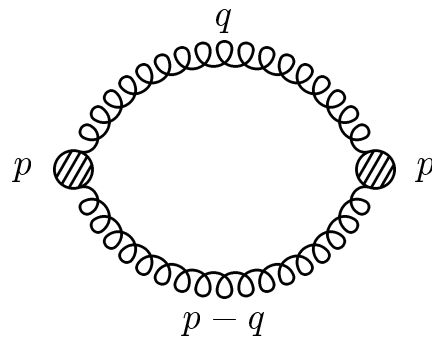


Figure 4

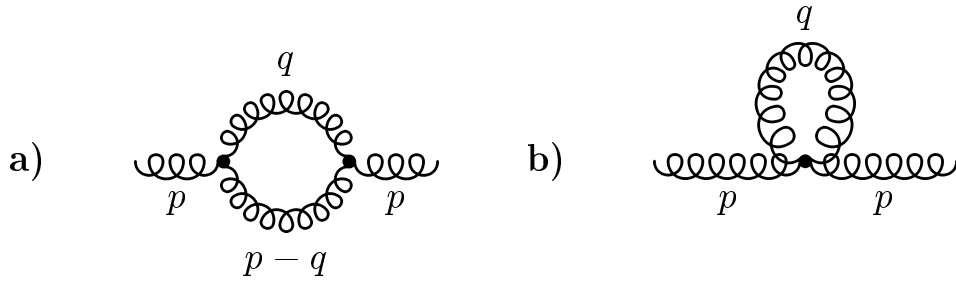


Figure 5

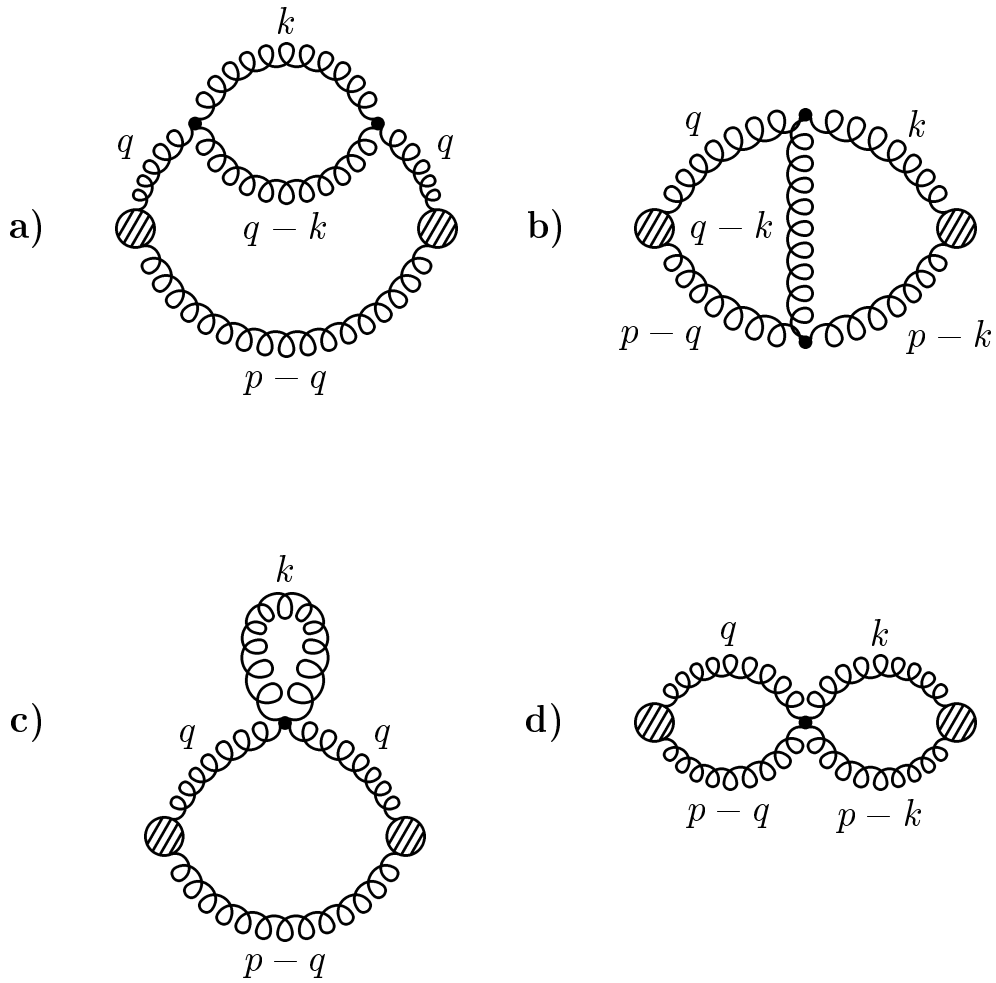


Figure 6

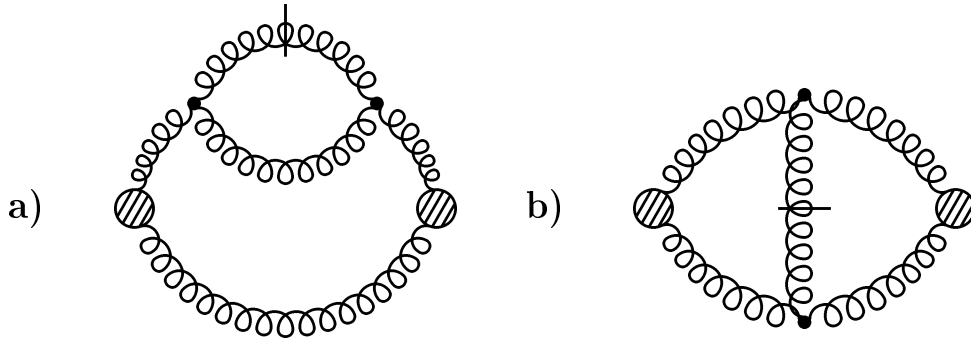


Figure 7

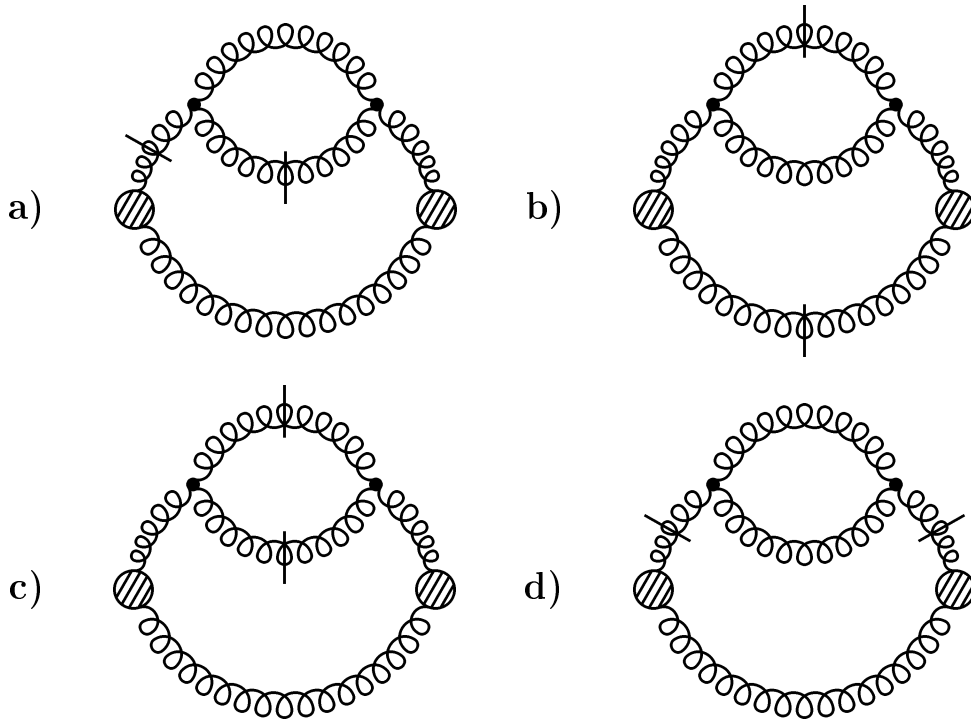


Figure 8

